CHARLES UNIVERSITY IN PRAGUE

Faculty of Science

Department of Physical and Macromolecular Chemistry

STUDIES OF LANTHANIDE COMPLEXES BY A COMBINATION OF SPECTROSCOPIC METHODS

Diploma Thesis

Monika Krupová

Supervisor: prof. RNDr. Petr Bouř, DSc.

Prague, 2014

Prohlášení:

Prohlašuji, že jsem závěrečnou práci zpracovala samostatně a že jsem uvedla všechny použité informační zdroje a literaturu. Tato práce ani její podstatná část nebyla předložena k získání jiného nebo stejného akademického titulu.

V Praze, ……..…… .....…….……

Podpis

Acknowledgements

I would like to thank my supervisor, prof. RNDr. Petr Bouř, DSc. for his time, patience, endless effort and help with my work. I greatly appreciate the trust he had given me and the opportunity to work and learn in a very stimulating environment. I would also like to thank to all of the members of Laboratory of Molecular Spectroscopy in IOCB AS CR for creation of a friendly environment and for their helpful remarks. Notably, my great appreciation goes to Valery Andrushchenko for his help with my experimental work.

ABSTRACT

Studies of Lanthanide Complexes by a Combination of Spectroscopic Methods

Monika Krupová

(Department of Physical and Macromoecular Chemistry, Faculty of Science, Charles University in Prague)

Since conventional structural analysis offers rather limited means for the chirality detection, a series of lanthanide tris-(*β*-diketonates) are investigated as effective receptors for a better chirality sensing in biomolecular substrates. These lanthanide complexes containing *β*-diketonate ligands are electrically neutral; they can further coordinate with various small organic molecules such as chiral alcohols, amino alcohols or amino acids in organic solvents and produce a strong chiral signal.

Previously, a resonance in Raman scattering was observed in the studied systems due to the correspondence of europium electronic transition energy to the laser excitation wavelength, about a 100-fold signal enhancement if compared to non-resonant vibrational ROA was observed. This enabled shorter detection times as well as lower sample concentrations.

In the current work, interaction of the Eu(FOD) complex with *(R)*- and *(S)*-enantiomer of 1-phenylethanol in n-hexane was studied using IR spectroscopy, Raman spectroscopy and Raman optical activity (ROA), UV-Vis spectroscopy and ultraviolet circular dichroism (UVCD). Only ROA and UVCD spectroscopies proved to be sensitive enough to the complexation of the studied chemical species.

The UVCD proved especially useful to support the results obtained by ROA measurements and determine the metal/ligand ratio in the complex. Although lanthanide tris-(*β*-diketonates) are silent in UVCD spectra, symmetric UVCD signals induced around 300 nm were observed for Eu(FOD) upon complexation with *(R)*- and *(S)*- 1-phenylethanol.

In the future, experiments with structural variations of lanthanide tris-(*β*-diketonate) complexes and theoretical modeling are planned to refine the chirality sensing systems for chiral recognition in biological substrates.

Key words: *Lanthanide Complexes, Europium, Raman Optical Activity, Resonance, Circular Dichroism, Quantum Mechanics, Chirality, Molecular Structure.*

ABSTRAKT

Studium komplexů lanthanoidů pomocí spektroskopických metod

Monika Krupová

(Katedra fyzikální a makromolekulární chemie, Přírodovědecká fakulta, Univerzita Karlova v Praze)

Konvenční strukturní analýza nabízí pouze omezené možnosti k určení absolutní konfigurace chirálních látek. Jednou z možností je použití komplexů lanthanoidů s tris-(*β*-diketonátovými) ligandy. Tyto komplexy jsou elektricky neutrální a v organických rozpouštědlech mohou tvořit jiné komplexy s různými malými organickými molekulami, např. s chirálními alkoholy a aminoalkoholy. Díky této interakci je pak možné chiroptickými metodami určit konfiguraci chirální látky.

Abychom interakci organická látka-Ln komplex lépe porozuměli, studovali jsme interakci komplexu Eu(FOD) s (*R*)- a (*S*)- enantiomerem 1-fenylethanolu (PE) v n-hexanu pomocí IR spektroskopie, Ramanovy spektroskopie, Ramanovy optické aktivity (ROA), UV-Vis absorpce a UV cirkulárního dichroismu (UVCD). Jenom ROA a UVCD spektra byly dostatečně citlivé pro studium komplexace zkoumaných systémů. S jejich pomocí se podařilo přibližně určit poměr kov/ligand v komplexu a vazebnou konstantu.

V předchozích experimentech bylo pozorováno stonásobné zvětšení ROA signálu, např. alkoholu v komplexu, oproti volné chirální látce. Je to částečně dáno rezonancí excitačního laserového záření s elektronickými přechody Eu^{3+} iontu. Díky tomu je možné výrazně snížit čas a zmenšit potřebnou koncentraci při změření ROA spektra. Data získaná pomocí Ramanovy optické aktivity byly podpořeny naměřením UVCD spekter. Komplex Eu(FOD) a PE indukoval přibližně symetrický UVCD signál v okolí 300 nm.

Domníváme se, že cíleným výběrem ligandů navázaných na Eu^{3+} iont by v budoucnu bylo možné zvýšit afinitu nebo selektivitu komplexů vůči různým chirálním substrátům. Zejména teoretické modelování by umožnilo lépe pochopit povahu interakce mezi Eu^{3+} komplexem a chirální molekulou, a vysvětlit mechanizmus rezonančního ROA.

Klíčová slova: *komplexy lanthanoidů, europium, Ramanova optická aktivita, rezonance, cirkulární dichroismus, kvantová mechanika, chiralita, molekulová struktura.*

CONTENT

ABBREVIATIONS

CID	*Circular Intensity Difference*
DCP	*Dual Circular Polarization*
Eu(FOD)	*europium tris(6,6,7,7,8,8,8-heptafluoro-2,2-dimethyloctane-3,5-dione)*
FA	*Factor Analysis*
ICP	*Incident Circular Polarization*
IR	*InfraRed*
IRROA	*Induced-Resonance Raman Optical Activity*
Ln	*Lanthanide*
NMR	*Nuclear Magnetic Resonance*
PE	*1-PhenylEthanol*
ROA	*Raman Optical Activity*
SCP	*Scattered Circular Polarization*
SVD	*Singular Value Decomposition*
UV	*UltraViolet*
UVCD	*UltraViolet Circular Dichroism*
VOA	*Vibrational Optical Activity*

1. INTRODUCTION

1.1. Symmetry of Molecules and Optical Activity

Objects that can be viewed as non-superimposable mirror images of each other are said to be chiral (Figure 01). A molecule is chiral only if it does not possess an axis of improper rotation S_n (a symmetry operation composed of two successive transformations – a rotation through 360°/n followed by a reflection through a plane perpendicular to the axis of rotation). Any molecule possessing a centre of inversion i is achiral, since $i = S_2$. Similarly, if a molecule possesses a mirror plane σ_h it is achiral, because $\sigma_h = S_1$.[/01/] Molecules that are chiral exist in two forms characterized by their mirror images called enantiomers. Chiral molecules are optically active, i.e. they can rotate the plane of linearly polarized light in equal but opposite directions.

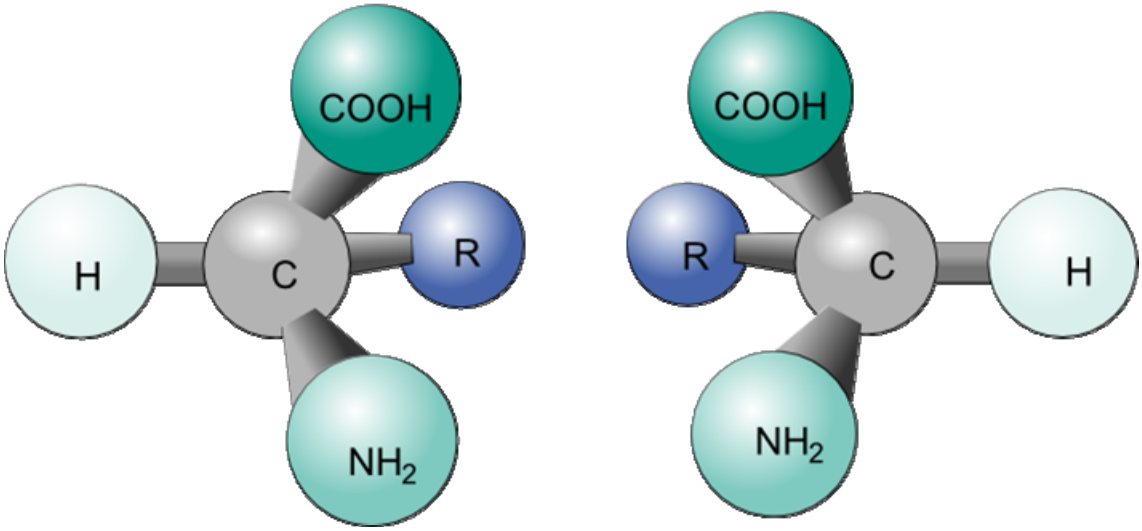

Figure 01. Chirality in molecules:[/02/] *Molecules are said to be chiral if their mirror images can not be superimposed. The most frequent chiral molecules contain assymetric carbon (carbon with 4 different substituents in a tetrahedral geometry). The absolute configuration of such molecules is assigned by the R/S notation, where we assign priority to substituents according to the Cahn-Ingold-Prelog rules.*[/03/]

Interestingly, enantiomers of chiral molecules are not energetically equivalent. The principle of conservation of parity proposed in 1927[/04/] postulated that all physical laws are invariant to spatial inversion through a coordinate origin. However, experiments concerned with β-decay showed that parity is violated by the weak nuclear force. Therefore,

fundamental particles have an intrinsic handedness. It was shown, that there is a nonzero enthalpy of reaction for stereomutation:

$$S = R.\Delta_r H_0^0 \approx N_A.\Delta_{PV} E \qquad [01]$$

where $\Delta_{PV}E$ is the parity-violating energy difference and N_A is the Avogadro constant.[/05/] This energy difference was predicted to be very small (~ 10^{-14} J.mol^{-1}) for most molecules,[/06, 07/] even though later simulations revealed that the absolute value of $\Delta_{PV}E$ can be sometimes by several orders of magnitude larger.[/05, 08/] This symmetry violation, however, thus does not account for observable differences of enantiomer properties when studied by contemporary spectroscopic methods.

In order to understand the nature of molecular response to the right- and left-circularly polarized light, we need to take into account several contributions regarding the interaction of the light wave with a chiral molecule. In addition to the electric dipole moment induced by the electric field of the light, it is necessary to incorporate the magnetic dipole moment and electric quadrupole moment.[/09/] These interactions are typically described by the dynamic (= frequency-dependant) molecular property tensors:

$$\alpha_{\alpha\beta} = \frac{2}{\hbar}\sum_{j\neq n}\frac{\omega}{\omega_{jn}^2-\omega^2}\,\mathrm{Re}\left(\langle n|\mu_\alpha|j\rangle\langle j|\mu_\beta|n\rangle\right) \qquad [02a]$$

$$G'_{\alpha\beta} = -\frac{2}{\hbar}\sum_{j\neq n}\frac{\omega}{\omega_{jn}^2-\omega^2}\,\mathrm{Im}\left(\langle n|\mu_\alpha|j\rangle\langle j|m_\beta|n\rangle\right) \qquad [02b]$$

$$A_{\alpha\gamma\beta} = \frac{2}{\hbar}\sum_{j\neq n}\frac{\omega}{\omega_{jn}^2-\omega^2}\,\mathrm{Re}\left(\langle n|\mu_\alpha|j\rangle\langle j|\Theta_{\beta\gamma}|n\rangle\right) \qquad [02c]$$

where $\alpha_{\alpha\beta}$ is the electric dipole – electric dipole polarizability, $G'_{\alpha\beta}$ is the electric dipole – magnetic dipole polarizability, and $A_{\alpha\beta\gamma}$ is electric dipole – electric quadrupole polarizability. Symbols n and j correspond to the initial and excited states of a molecule, and ω_{jn} is their angular frequency separation, ω is the angular frequency of the incident radiation, and $\hbar$ is the reduced Planck's constant. Operators of cartesian components of the electric dipole moment, magnetic dipole moment and electric quadrupole moment are symbolized by μ_α, m_α and $\Theta_{\alpha\beta}$, respectively. [/09, 10/]

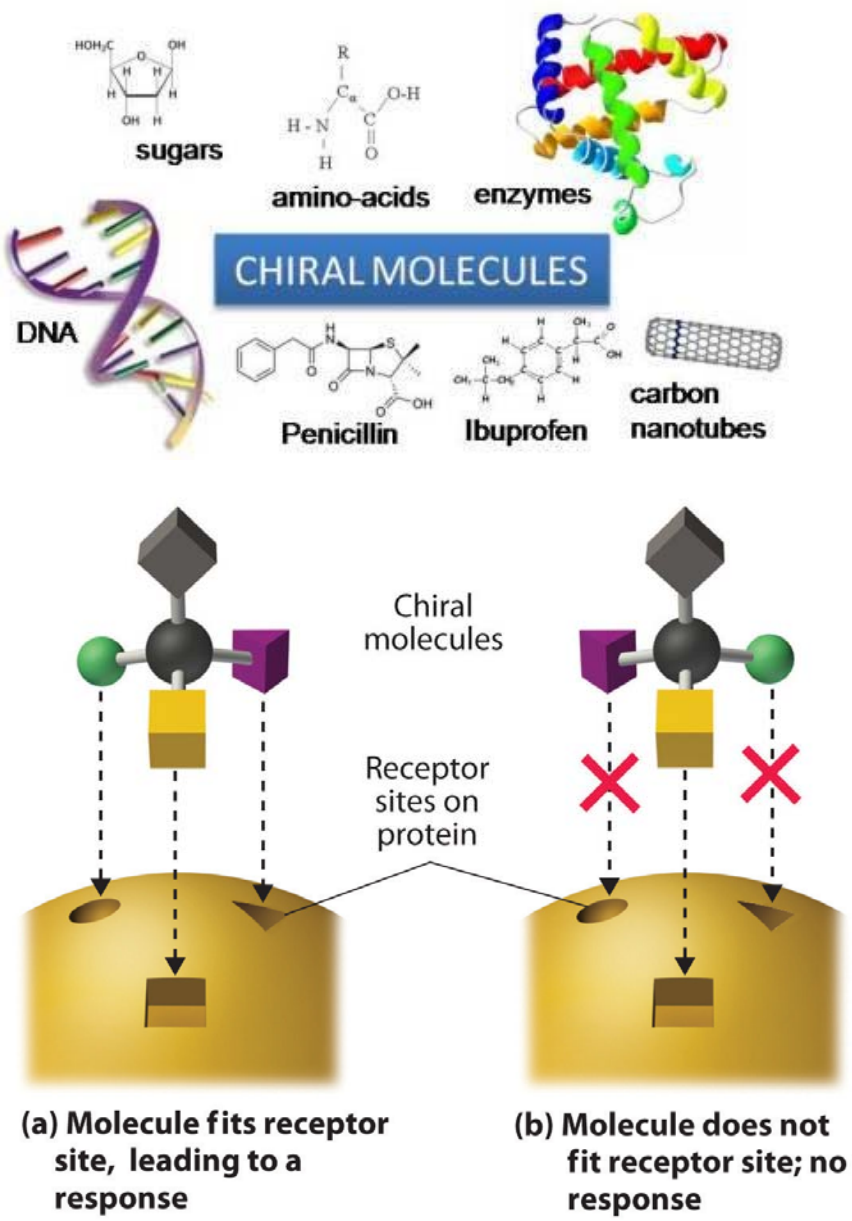

Figure 2. Chirality in biology:[11, 12] *Many molecules constituting building blocks of life as well as metabolites and substrates for biochemical reactions are chiral (top part of the Figure). This has several important consequences, such as the enantiomeric specificity of enzymes and receptors towards substrates (bottom part of the Figure).*

Chirality of molecules leads to the necessity of absolute configuration determination in various fields of chemistry, organic synthesis[13], medicine or material sciences. The importance of chiral recognition is particularly evident in biological and life sciences (Figure 2). Basic building blocks of biological macromolecules (e.g. amino acids) are chiral with only one specific enantiomer preffered. In some cases, one enantiomer of a

chiral molecule is extremely important for the biochemical processes while the other enantiomer is ineffective, or even harmful.[14, 15]

1.2. Methods Used for Chirality Determination

The main advantage of chiroptical spectroscopic techniques is their ability to easily determine absolute configuration due to the opposite spectral pattern of the enantiomers. They are easy to apply and accessible for a wide range of chemical compounds in their natural environment. Optical rotatory dispersion (ORD) and ultraviolet circular dichroism (UVCD) have been used for many years, even though the use of UVCD is limited to molecules with active chromophores. Recently, vibrational spectroscopic techniques such as vibrational circular dichroism (VCD) and Raman optical activity (ROA) started to prevail for chirality detection. Since a vibrational spectrum contains more bands sensitive to the detailed molecular structure ($3N - 6$ fundamentals, where N is the number of atoms in the molecule), vibrational spectrum of chiral compounds can provide more detailed stereochemical information than the electronic one.[09]

1.2.1. Optical Rotatory Dispersion

The electric vector $\vec{E}$ of linearly polarized light can be described as a superposition of two vectors $\vec{E}_L$ and $\vec{E}_R$ of equal magnitude that are rotating in the opposite directions (eq. 03). Conventionally, $\vec{E}_L$ corresponds to vector that rotates counter-clockwise when looking towards the light source, and $\vec{E}_R$ corresponds to a clockwise rotating vector. A linearly polarized wave can be thus considered a superposition of a right- and left-handed circularly polarized wave of the same frequency and phase.

$$\vec{E} = \vec{E}_L + \vec{E}_R \qquad [03]$$

When a light wave enters an optically active environment, refractive indices for left- and right-handed circularly polarized light may differ (eq. 04), their electric field vectors then rotate at different speeds. Their superposition still yields a linearly polarized light, but its polarization plane is rotated by an angle α (eq. 05).

$$n_L \neq n_R \qquad [04]$$

$$\alpha = \frac{180}{\lambda}(n_L - n_R).d \qquad [05]$$

The angle of rotation α is proportional to the difference of the refractive indices for the left- and right-handed circularly polarized light $n_L - n_R$, and to the distance travelled in the optically active medium d. λ is the wavelength of the light.[16] Relations between the quantities mentioned above are summarized in table 1.

Right-handed Rotation	Left-handed Rotation
$n_L > n_R$	$n_L < n_R$
$v_L < v_R$	$v_L > v_R$
$\alpha > 0$	$\alpha < 0$
So called dextrorotatory (+)	So called laevorotatory (-)

Table 1. Relations between quantities describing optical rotation: *n_L and n_R corresponds to the refractive indices of left- and right-circularly polarized light, respectively. Similarly v_L and v_R are their speeds of propagation, and α is the angle of rotation.*

As seen in eq. 05, optical rotation is also dependent on the wavelength of the incident polarized light λ. This dependance is called the optical rotatory dispersion. ORD found its use already in the middle of the 20th century in absolute configuration determinations of simple organic and biological molecules, and in predictions of the structure of bigger biological systems such as polypeptides and polynucleotides.[17, 18] To some extent, this technique was later substituted by other spectroscopic methods such as UVCD, and vibrational optical activity (VOA), i.e. VCD and ROA.

1.2.2. Ultraviolet Circular Dichroism

Ultraviolet Circular Dichroism is closely linked to ORD, but its spectra are closer related to molecular structure. When light passes through optically active environment, not only the refractive indices for the right- and left-circularly polarized light differ (eq. 04), but also the absorption of right and left-circularly polarized light (A_R and A_L, respectively) is different (eq. 06). According to the Lambert-Beer law, absorption of the samples is proportional to the concentration c and the length of the cuvette l by the extinction

coefficient ε (eq. 07). In UVCD, the difference of extinction coefficients for left- and right-circularly polarized light, ε_L and ε_R, respectively, is measured (eq. 09). I_0 symbolizes the intensity of the incident light, I is the intensity of the transmitted light after passing through the absorbing environment.[19, 20]

$$A_L \neq A_R \qquad [06]$$

$$\varepsilon = \frac{-\log \frac{I}{I_0}}{l.c} \qquad [07]$$

$$\text{where } -\log \frac{I}{I_0} = A$$

$$I_L \neq I_R \qquad [08]$$

$$\Delta\varepsilon = \varepsilon_R - \varepsilon_L \qquad [09]$$

The dependence of $\Delta\varepsilon$ on the wavelength of the incident light λ is the CD spectrum of the sample. CD spectrum is often expressed as the molar ellipticity [θ]. The intensities of the right- and left-handed circularly polarized light (I_R and I_L, respectively) after passing through the absorbing optically active environment are different (eq. 08). The tip of $\vec{E}$ moves along an ellipse and elliptically polarized light is obtained (Figure 3, page 14).

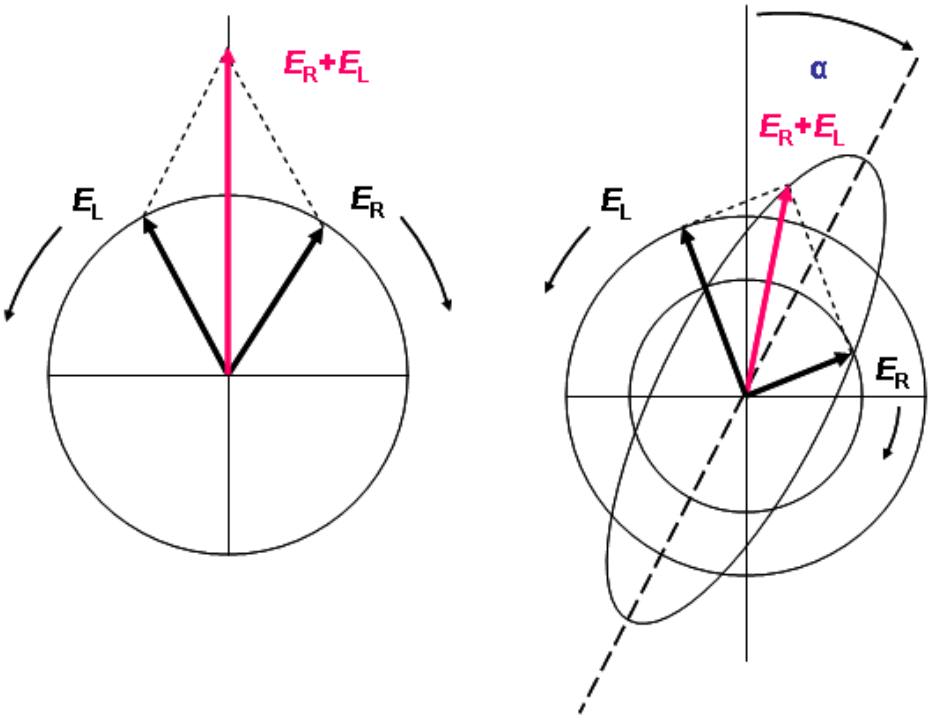

Figure 3. Optical rotation and elliptical light:[21] *The electric vector E of linearly polarized light is a superposition of vectors E_L and E_R of equal magnitude rotating in opposite directions (left). If light passes through absorbing optically active environment, the vectors E_L and E_R not only rotate at different speeds, but also have a different magnitude. Superposition of these two vectors then yields the elliptically polarized light (right).*

This ellipticity is quantified by the angle $[\theta]$ given by equation 10. Symbols oA and oB correspond to the semimajor and semiminor axes of the ellipse, respectively. The relation of $[\theta]$ and $\Delta\varepsilon$ is defined by equation 11.[20]

$$tg[\theta] = \frac{oB}{oA} \qquad [10]$$

$$[\theta] = 3300.\Delta\varepsilon \qquad [11]$$

Chiral molecule active in UVCD spectra needs to absorb light in UV and Vis spectral region (e.g.~ 180 – 800 nm). UVCD is very popular in the estimation of protein secondary structure as there are several UVCD active bands in each protein. Bands in far-UV region correspond to the absorption of peptide bonds and the UVCD shape is dependent on the secondary structure of the polypeptide main chain. Aromatic and

disulfide chromophores (e.g. sidechains of tyrosine, histidine, tryptophane, phenylalanine and -S-S- of cystine) induce UVCD signal within 245 – 300 nm and account for conformational changes in the tertiary structure of a protein as well.[20]

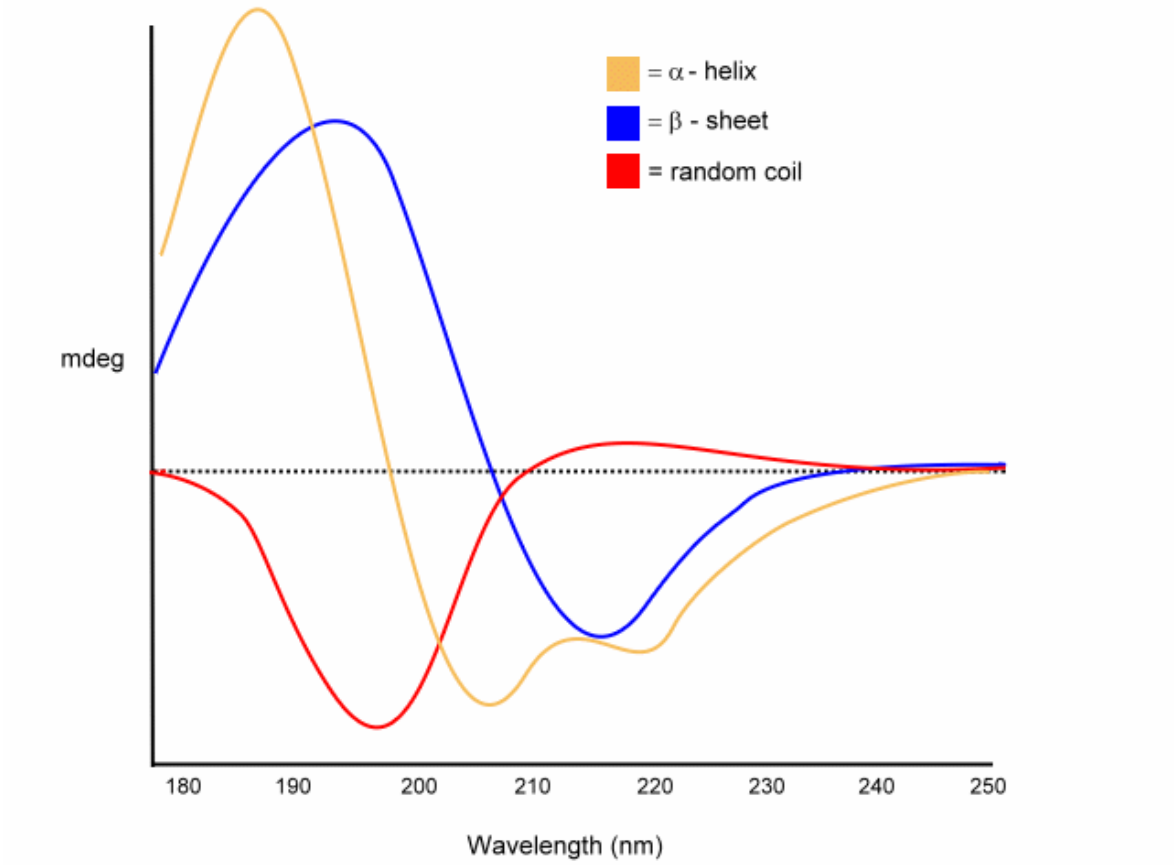

Figure 4. Average UVCD patterns of three secondary structure types of proteins:[22] *When estimating their content, the experimental UVCD curve is fitted as a superposition of these 3 model curves. The parameters of the fit give the approximate conformational ratios.*

Typical UVCD spectral patterns for individual secondary structures are shown in Figure 4. Nowadays, the estimation of protein secondary structure from CD spectra is implemented in many software packages[23] and even on-line analysis of UVCD spectroscopic data for proteins providing the secondary structure content is available (e.g. DICHROWEB).[24, 25]

1.2.3. Vibrational Circular Dichroism

Another technique that can provide molecular stereochemistry information concerning the structure, conformation and absolute configuration is vibrational circular dichroism (VCD). First VCD experiments were published in mid 1970s'.[26, 27] Not long

after, VCD advantages could be appreciated. Unlike UVCD, VCD provides more bands. Moreover, investigated molecules do not need to have a chromophore active in UV. Finally, the probability of incorrect interpretation of VCD spectra is smaller than in the case of UVCD spectroscopy.[28]

VCD is the difference in absorption of left- and right-circularly polarized IR radiation:

$$\Delta A = A_L - A_R \qquad [12]$$

Infrared absorption depends on the dipole strength D_{jn}, while the differential absorption is proportional to the rotational strength R_{jn}. For a transition $n \longrightarrow j$, the dipole and rotational strengths are:

$$D_{jn} = \mathrm{Re}\left\{\langle n|\mu|j\rangle.\langle j|\mu|n\rangle\right\} \qquad [13a]$$

$$R_{jn} = \mathrm{Im}\left\{\langle n|\mu|j\rangle.\langle j|m|n\rangle\right\} \qquad [13b]$$

Using these two quantities, we can define Kuhn's dissymmetry factor:[09, 29]

$$2\frac{\varepsilon_L - \varepsilon_R}{(\varepsilon_L + \varepsilon_R)} = \frac{4R_{jn}}{cD_{jn}} \qquad [14]$$

where ε_L and ε_R are the extinction coefficients for left- and right-circularly polarized light, respectively, and c is the speed of light in vacuum. The same principles apply for UVCD discussed above.

Application of VCD to studies of conformations of biomolecules, mainly peptides and proteins, are quite interesting. Three so called *amide bands* are the most important. The *amide I* mode is the most characteristic and the most intense vibration of proteins in IR and VCD spectra and it originates mainly in the C=O stretching vibration. The *amide II* mode refers to the in-plane N-H bending with some C-N stretching contribution, and so does the *amide III* mode which is usually very weak in VCD spectra.[30] The shape and location of these bands reflect local conformation of the amino acid residues (characterized by the φ

and ψ dihedral angles), coupling of neighboring amide groups, and frequency shifts caused by the H-bonding dependent on the secondary structure of polypeptides and proteins.[28]

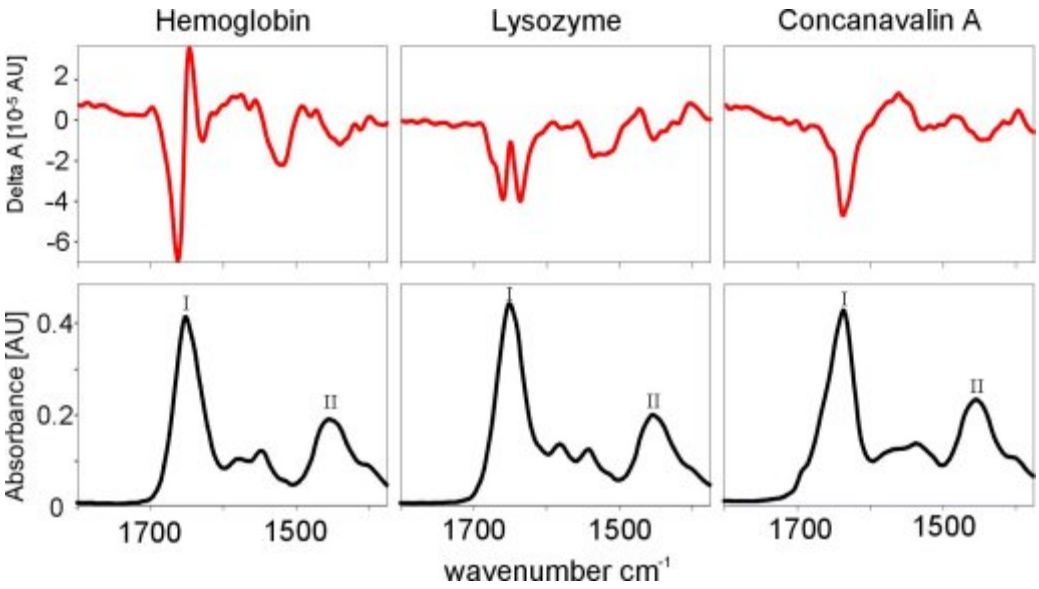

Figure 5. IR and VCD spectra of three proteins with different secondary structures:[31] *At the top, VCD spectra of the proteins are shown. The bottom panel shows the IR spectra. Hemoglobin is typical for a high content of the α-helical secondary structure. On the other hand, concanavalin A consists mainly of β-sheets. Lysozyme has about the same ratio of α-helical and β-sheet secondary structures.*

Empirical rules for prediction of the periodic secondary structures (e.g. α-helix, 3_{10}-helix, β-sheet) were based on the analysis of a large number of proteins. Known structure (obtained by X-ray crystallography or NMR) was correlated with their VCD spectra. For example, while right-handed α-helical and 3_{10}-helical structures account for a positive *amide I* and negative *amide II* couplet in VCD spectra (centered at~ 1650 cm^{-1}), left-handed helices and unordered secondary structures are characterized by a negative *amide I* couplet. Similarly, the presence of β-sheets in the structure of a protein molecule is indicated by a weak negative *amide I* VCD band at around 1630 cm^{-1}.[32] This was rationalized by ab initio predictions of protein VCD.[33]

1.2.1. Raman Optical Activity

The theory of Raman scattering from chiral molecules was introduced in the end of 1960s'.[34] The first observations of this phenomenon in 1973[35] were soon followed by extensive technical, experimental and theoretical progress in the field. Raman optical

activity is the difference in intensity of the right- and left-circularly polarized light scattered by a chiral molecule (eq. 15). There are different approaches to ROA spectra measurements – incident circular polarization (ICP), dual-polarization (DCP) and scattered circular polarization (SCP). In the case of the ICP and SCP mode, circular intensity difference (CID) can be defined using equation 16.

$$I^R \neq I^L \qquad [15]$$

$$CID = \frac{I^R - I^L}{I^R + I^L} \qquad [16]$$

Symbols I^R and I^L correspond to the scattered intensities of right- and left-circularly polarized incident light, respectively. In the SCP mode, linearly polarized incident light causes a small circularly polarized component in the scattered beam when interacting with a chiral compound.

Several experimental configurations are possible. The angle at which the scattered light is observed can be varied from forward (0°), right-angle (90°) to backward (180°) direction. If the scattering is observed in right angle, two distinct ICP measurements can be distinguished. If the polarization analyzer in the scattered beam with its transmission axis is perpendicular to the scattering plane, we are speaking of polarized ROA. In case of depolarized ROA, this geometry is parallel to scattering plane./09/ Dual circular polarization (DCP) refers to technique where both the incident and the scattered light are circularly polarized./36, 37/

Selection rules for natural vibrational ROA are given by components of $\alpha_{\alpha\beta}$, $A_{\alpha\beta\gamma}$ and $G'_{\alpha\beta}$. Following expressions can be written for CIDs associated with individual scattering geometries:/09, 38/

$$CID(180°) = \frac{48\left[\beta G' + \frac{1}{3}\beta(A)^2\right]}{2c\left[45\alpha^2 + 7\beta(\alpha)^2\right]} \qquad (04a)$$

$$CID_x(90°) = \frac{12\left[45\alpha G' + 7\beta(G')^2 + \beta(A)^2\right]}{c\left[45\alpha^2 + 7\beta(\alpha)^2\right]} \qquad (04b)$$

$$CID_y(90°) = \frac{12\left[\beta(G')^2 - \frac{1}{3}\beta(A)^2\right]}{6c\beta(\alpha)^2} \tag{04c}$$

$$CID(0°) = \frac{8\left[45\alpha G' + \beta(G')^2 - \beta(A)^2\right]}{2c\left[45\alpha^2 + 7\beta(\alpha)^2\right]} \tag{04d}$$

where α and G' are so called isotropic invariants and $\beta(A)^2$, $\beta(\alpha)^2$ and $\beta(G')^2$ anisotropic invariants.[09]

$$\alpha = \frac{1}{3}\alpha_{\alpha\alpha} \tag{05a}$$

$$G' = \frac{1}{3}G'_{\alpha\alpha} \tag{05b}$$

$$\beta(G')^2 = \frac{1}{2}(3\alpha_{\alpha\beta}G'_{\alpha\beta} - \alpha_{\alpha\alpha}G'_{\beta\beta}) \tag{05c}$$

$$\beta(A)^2 = \frac{1}{2}\omega\alpha_{\alpha\beta}\varepsilon_{\alpha\gamma\delta}A_{\gamma\delta\beta} \tag{05d}$$

$$\beta(\alpha)^2 = \frac{1}{2}(3\alpha_{\alpha\beta}\alpha_{\alpha\beta} - \alpha_{\alpha\alpha}\alpha_{\beta\beta}) \tag{05e}$$

ROA found applications in many fields. It monitors conformational transitions in small chiral organic molecules as well as in large biomolecular systems. Specifically proteins are convenient to study by ROA, since signals dominating the ROA spectrum are characteristic of the backbone conformation.[09] For example, UVCD is not sensitive to *β*-turns. On the other hand, ROA seems to be promising for *β*-turn detection in protein molecules (Figure 6).[39]

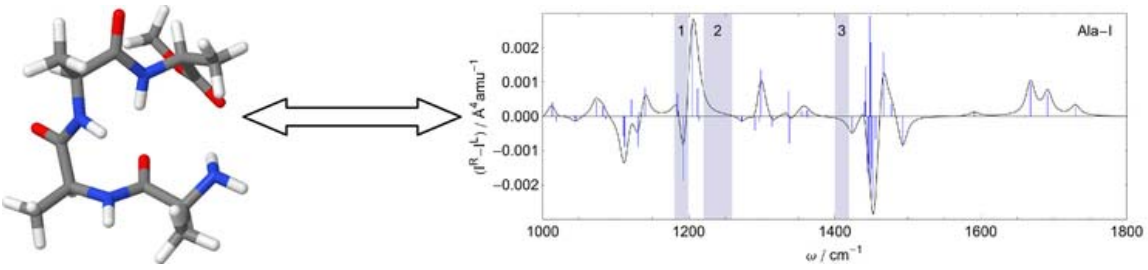

Figure 6. β-turns in proteins and Raman optical activity:[39] *Structure-spectra correlations for proteins showed that ROA can be a valuable tool in detection of β-turns in the protein structure.*

Even though ROA cannot provide as detailed structural information as the X-ray diffraction, the measurement can be carried out in aqueous solution to reflect the natural biological environment. Enantiomeric excess can be determined with a great accuracy (~ 0.1 %).[40] However, CID for a chiral molecule is in principle very small and this leads to long measurement times and high sample concentrations. Induced resonance ROA (IRROA) can overcome these setbacks and significantly decrease time as well as the sample concentrations.

1.2.1.1. ROA Instrumentation

In our experiment, we used a ROA spectrophotometer operating in the SCP mode with 180° configuration. A laser beam of 532 nm is produced and conducted through the optics to the sample compartment. Scattered light is then collected by polarization beam splitter that separates right- and left-circularly polarized components of the backscattered light. These two components are conducted by fiber optics into the spectrograph with a CCD detector. Software subtraction then provides the required SCP ROA.

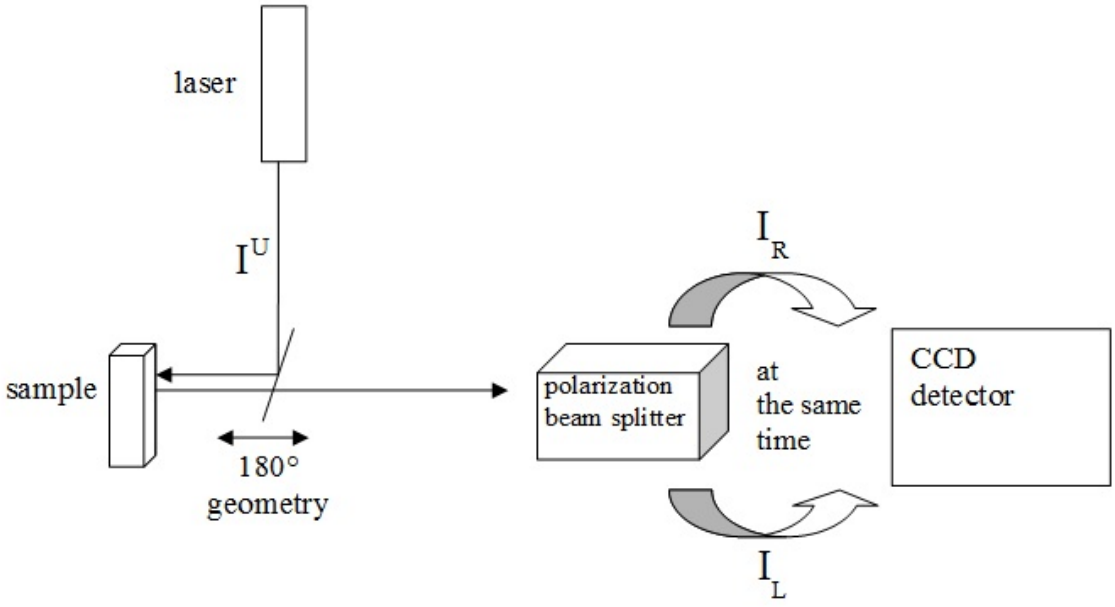

Figure 7. ROA spectrophotometer:[41] *SCP mode with 180° geometry is shown. Laser light produces linearly polarized beam at 532 nm* I^U *which is then conducted into the sample compartment. Raman backscattering is collected with polarization beam splitter, and separated right- and left-circularly polarized light (*I_R *and* I_L*, respectively) is then detected by CCD detector.*

1.3. Molecular Recognition via Lanthanide Coordination Chemistry

Lanthanide series of chemical elements contains 15 metallic elements with atomic numbers 57 – 71 composing a first row at the bottom of the periodic table (Figure 8). Lanthanides are *f*-block elements and they fill *4f* electron subshell. They typically form 3+ ions, even though 2+ and 4+ species are stable in some cases. One of the interesting features of the lanthanide ions is a regular decrease in size of the 3+ ions when progressing through the series known as lanthanide contraction. It is resulting from the increasing nuclear charge coupled with the ineffective screening of the *4f* levels. The decrease in size of 3+ ions of the lanthanides is also a factor in stability of the complexes of these ions. Complexes with a given ligand usually show increased stability when progressing through the series. Large coordination numbers (6 and more) are typical for lanthanides due to the ionic nature of the *lanthanide – ligand* bonds and due to the relatively large radii of the elements.[/42/] If small monovalent ligands are involved, high symmetry complexes are obtained (D_{3h}, C_{3v}). On the other hand, low symmetry is obtained (D_3 or lower) if bulky polyvalent ligands are coordinated. Coordination number 10 is also very common, but low symmetries C_1, C_2 or D_2 are usually obtained in this case.[/43/]

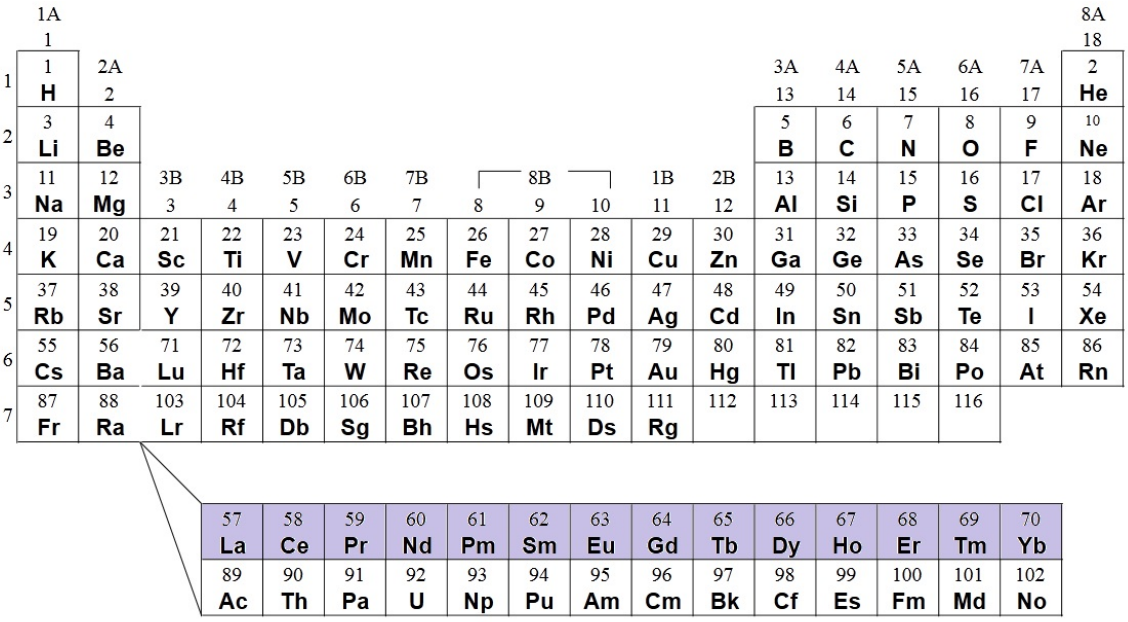

Figure 8. Periodic table and Lanthanides: *Lanthanides comprise of 15 metallic elements from Lanthanum through Cerium, Praseodymium, Neodymium, Promethium, Samarium, Europium, Gadolinium, Terbium, Dysprosium, Holmium, Erbium, Thulium, to Ytterbium (violet boxes).*

Ionic bonding interactions between Ln^{3+} ion and negatively charged donor groups are the basis of the lanthanide coordination. Therefore lanthanide complexes are characterized by a strong preference for negatively charged donor groups or strong chelating ligands such as compounds containing oxygen. The preference of Ln^{3+} ions for highly electronegative donors can be explained by the hybridization. The rare earth metal ions in general differ from each other in the number of electrons in the *4f* orbitals which are effectively shielded from interaction with ligand orbitals by the electrons in the *5s* and *5p* orbitals. Therefore unoccupied higher-energy orbitals such as *5d*, *6s* or *6p* must be involved if hybridization is to occur. This type of hybridization can be expected only due to the interaction with the most strongly coordinating ligands./44, 45/

The complexes are usually very weak. Since water molecules can compete with other ligands, all reagents and solvents must be water-free./46/ When the lanthanide cation is unsaturated, additional neutral or anionic substrate coordinates with the lanthanide center forming a *highly coordinated complex*. The additional coordination has a great influence on the geometrical arrangements of the ligands. Proper combination of lanthanide center and original ligand can control the complex formation with a specific substrate./14/

Several types of lanthanide complexes have been successfully used as functional molecular probes in chemistry, biology, medicine and material science. Catalysts of organic and biological reactions, nuclear magnetic resonance probes,/47, 48, 49/ and luminescent sensors/50/ are among the most significant applications of lanthanide coordination chemistry. Lately, their role in chirality sensing of biological substrates was extensively studied. The main idea of chirality sensing via lanthanide coordination chemistry is based on the fact that when a lanthanide cation or complex couples with a chiral substrate, specific interactions occur in the lanthanide coordination sphere. These interactions induce chirality dependent changes that are detectable by spectroscopic techniques./14/ Experiments showed that by design of ligands in Ln^{3+} coordination sphere, lanthanide complexes are quite potent in enantioselective extraction of unprotected amino acids from neutral aqueous solvents/51/, or in determination of absolute configuration of biological substrates via NMR, UVCD and CPL spectroscopic methods./52, 53/

2. OBJECTIVES OF THE WORK

The aim of this work was to study an interaction of europium tris(6,6,7,7,8,8,8-heptafluoro-2,2-dimethyloctane-3,5-dione) with a simple chiral organic molecule 1-phenylethanol. In the course of our work, a stability constant for **η** = 1:1 (**η** = PE / Eu(FOD) concentration ratio) complex should be determined. Factor analysis is to be employed to process spectroscopic data. The nature of this interaction was studied using the following spectroscopic methods:

- UV-Vis Absorption Spectroscopy
- Ultraviolet Circular Dichroism
- Raman Scattering
- Raman Optical Activity
- Infrared Spectroscopy

3. EXPERIMENTAL

3.1. Material

3.1.1. Technical equipment

- BioTools ROA spectrophotometer ChiralRAMAN-2X
  BioTools, Inc. (USA)
- CD spectropolarimeter Jasco J-815
  Jasco, Inc. (Japan)
- UV-VIS-NIR spectrophotometer Varian Cary 500
  Varian, Inc. (USA)
- IR spectrophotometer Nicolet 6700
  Thermo Fisher Scientific, Inc. (USA)
- Analytical Scale
- *Typical laboratory equipment such as test tubes, eppendorf tubes, automatic pipettes, glass bottles, etc. was used. Quartz cuvettes for UV-Vis absorption and UVCD experiments were used, NaCl cell was used to perform IR experiment.*

3.1.2. Chemicals

- Europium tris(6,6,7,7,8,8,8-heptafluoro-
  -2,2-dimethyloctane-3,5-dione)
  Obtained from Sigma-Aldrich Co. LLC (USA) as Resolve-Al Eu(FOD) in 99% quality.

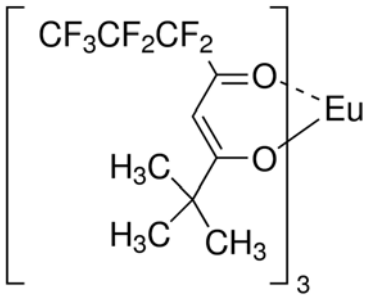

- 1-Phenylethanol

  Both (S-) and (R-) enantiomers of 1-Phenylethanol were obtained from Sigma-Aldrich Co. LLC (USA) in 98% quality.

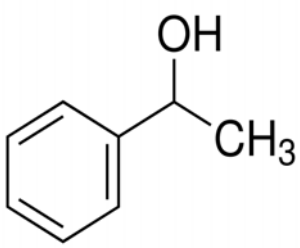

- n-Hexane

  n-Hexane obtained from Penta, s.r.o. (Czech Republic) in p.a. purity was used as a solvent in the experiments. Since ambiguity about its dryness emerged, it was dried over Na metal according to standard protocols, even though this action did not seem to affect the results of the experiments.

3.2. General methods

3.2.1. UV-Vis Absorption Spectroscopy

UV-Vis absorption experiment was performed on UV-VIS-NIR spectrophotometer *Varian Cary 500* in double beam mode. All experiments were performed at room temperature (~ 25 ºC) with pure n-hexane in the reference cell. Two different approaches were used – either solution with constant Eu(FOD) concentration was titrated by concentrated PE solution, or solution with constant PE concentration was titrated by concentrated Eu(FOD) solution.

In the first case, Eu(FOD) was dissolved in n-hexane so that the Eu(FOD) concentration in the resulting solution was 25 μmol.dm^{-3}. 2 ml of this solution were loaded into quartz cuvette and placed in the instrument. Concentration of PE in the sample (and therefore the ratio of PE / Eu(FOD) = **η**) was varied by subsequent additions of 10 μl of concentrated PE solution, therefore giving **η** = 1 for 1st addition, **η** = 2 for 2nd addition, and so on. UV-Vis absorption spectra were collected within 200 – 800 nm, but strong absorption was recorded only under 400 nm. Therefore further spectra were collected within 200 – 400 nm.

When PE concentration in the solution was held constant and Eu(FOD) concentration varied, 2 ml of 0.25μM PE solution were loaded into quartz cuvette and placed into the sample cell holder of the instrument. This solution was titrated with subsequent additions of 10 μl of concentrated Eu(FOD) so that the desired **η** was reached and UV-Vis absorption spectra were collected.

3.2.2. Ultraviolet Circular Dichroism

Ultraviolet circular dichroism titration experiment was performed using CD spectropolarimeter *Jasco J-815* at room temperature (~ 25 ºC). Separate samples of Eu(FOD) / PE mixtures dissolved in n-hexane were prepared, sufficient volume (~ 200 µl) of the samples was loaded into 0.2cm thick quartz cuvette and CD spectra were collected. Eu(FOD) concentration in all of the samples was held constant (50 µmol.dm^{-3}) and PE concentration varied according to the desired **η**. Solvent background was subtracted and spectra were smoothed by a polynomial fit.

3.2.3. Raman Scattering and Raman Optical Activity

Raman scattering and Raman optical activity experiment was performed on the ROA spectrophotometer *ChiralRAMAN-2X* at room temperature (~ 25 ºC) using laser excitation of 532 nm. Separate samples of Eu(FOD) / PE mixtures dissolved in n-hexane were prepared so that the concentration of Eu(FOD) in the samples was 1 mmol.dm^{-3} and concentration of PE varied within 1 – 16 mmol.dm^{-3} according to the desired **η**. The sample solution in the volume of~ 100 µl was loaded into glass cuvette and placed into the instrument. Laser excitation wavelength was 532 nm and its power was set to 30 mW. Exposure time for each spectrum was 20 min. and spectra were collected with the resolution of 7 cm^{-1}. Solvent background was subtracted and spectra were smoothed using the third-order five-points Savitzky-Golay smoothing.

3.2.4. Infrared Spectroscopy

IR spectra of the samples with different PE / Eu(FOD) concentration ratios in n-hexane were recorded using IR spectrophotometer *Nicolet 6700*. Separate samples with constant Eu(FOD) concentration (5 mmol.dm^{-3}) and varying PE concentration (5 – 50 mmol.dm^{-3}) in n-hexane were prepared, so that the desired **η** was from 0.2:1 to 6:1. Sufficient volume (~ 60 µl) of these solutions was loaded into NaCl cells and IR spectra within 400 – 4000 cm^{-1} at room temperature (~ 25 ºC) were recorded. Solvent background was subtracted and spectra were smoothed using polynomial smoothing.

4. RESULTS

We conducted titration experiments involving mixtures of Eu(FOD) and both *(R)*- and *(S)*- enantiomers of 1-phenylEthanol in n-hexane followed by spectroscopic analysis. The dependence of spectral parameters on the concentration ratios (or **η**; **η** = PE / Eu(FOD) concentration ratio) was analyzed to reveal the nature of the *Eu – ligand* interaction.

Several spectroscopic techniques such as UV-Vis spectroscopy, ultraviolet circular dichroism, infrared spectroscopy, Raman scattering and Raman optical activity were used. Only ultraviolet circular dichroism and Raman optical activity proved to be sensitive enough to the complexation and gave usable results (see sections 4.2. and 4.3.). The spectra obtained by these two methods were subjected to the factor analysis using the algorithm of singular value decomposition (see section 4.2.1. and 4.3.1.).

4.1. UV-Vis Spectroscopy of Eu(FOD) / 1-Phenylethanol

UV-Vis absorption spectra of samples containing different Eu(FOD) to 1-phenylethanol concentration ratios dissolved in n-hexane were measured. Since a strong absorption was observed only under 400 nm, the wavelength range of 200 – 400 nm was collected and analyzed.

Concentrated *S*-1-Phenylethanol solution was added to the 2ml of Eu(FOD) solution (figure 9, part A; page 28). When the Eu(FOD) concentration was held constant (2.5×10^{-5} mol.dm^{-3}) and the concentration of *(S)*- enantiomer of PE changed, a slight shrink of the intensity of 291nm peak was observed. This was explained by the dilution of the sample. With increasing *S*-PE / Eu(FOD) concentration ratio, a red shift was observed for the absorption around 210 nm and below. This phenomenon, however, was not used because it occurred close to the inaccessible far UV region.

Similar experiments with constant *S*-1-phenylethanol concentration was performed (figure 9, part B; page 28). In this case a 0.25mM solution of *S*-PE in n-hexane was titrated with concentrated Eu(FOD) and UV-Vis absorption spectra in the wavelength range of 220 – 360 nm were collected. The intensity of the 291 nm peak corresponding to europium electronic transitions has been growing linearly with the concentration of Eu(FOD).

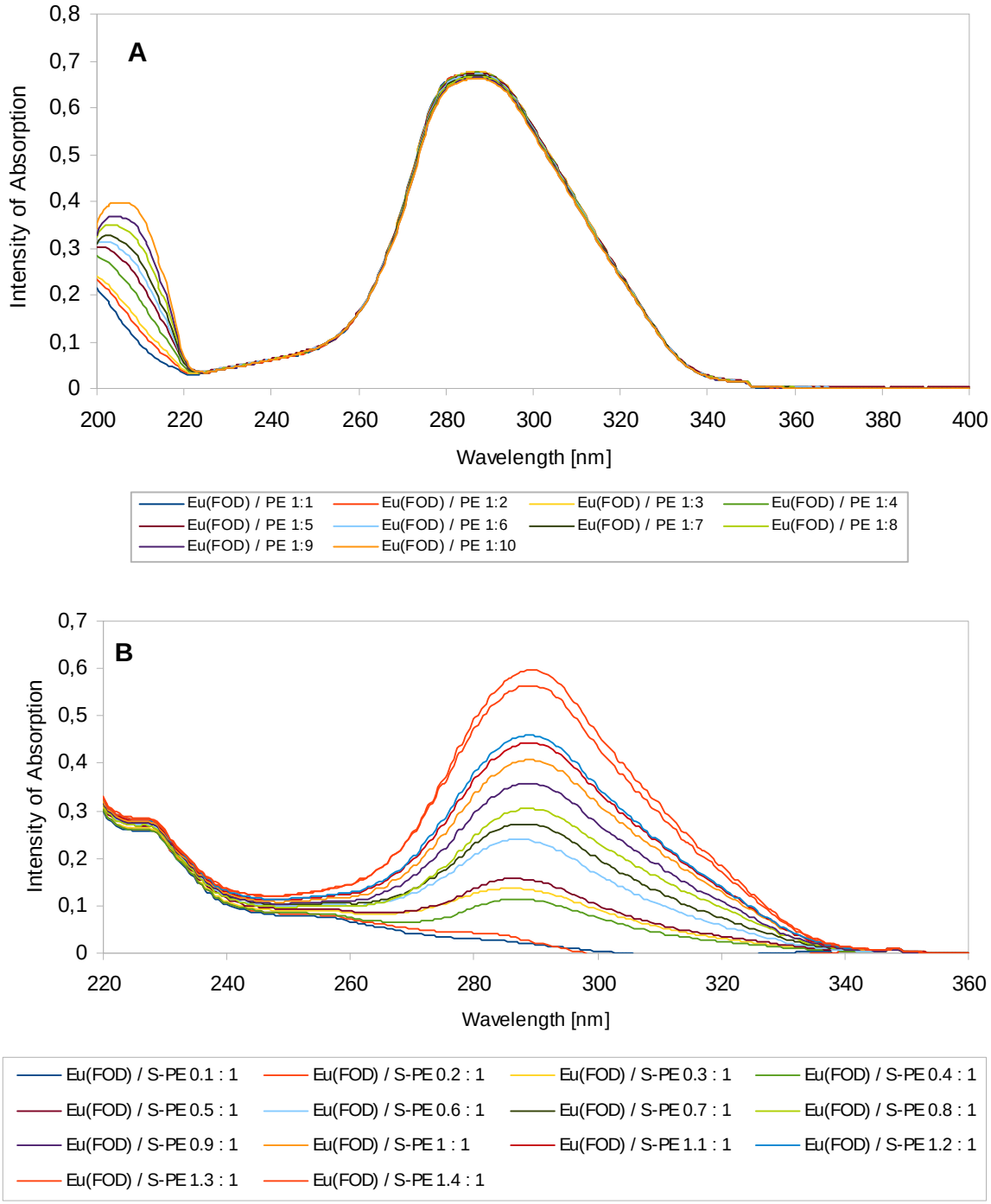

Figure 9. UV-Vis absorption spectra of Eu(FOD) and 1-phenylethanol mixtures in n-hexane: ***A:*** *0.025mM solution of Eu(FOD) was titrated with appropriate amount of concentrated S-PE to reach the desired* ***η****.* ***B:*** *0.25mM solution of S-PE was titrated with appropriate amount of concentrated Eu(FOD) solution so that the desired* ***η*** *was reached.*

4.2. Circular Dichroism of Eu(FOD) / 1-Phenylthanol

Ultraviolet circular dichroism (UVCD) was employed to study the interactions in the complex. Even though 1-phenylethanol can induce a typical three-peak UVCD signal within 240 – 270 nm, many other biologically relevant molecules lack chromophores or structural units with usable electronic transition frequencies. Therefore, the complexation of non-chromophoric chiral substrate to a metal ion providing electronic transitions in the accessible range seems to be promising for molecular chirality determination via chirality transfer.

A strong nearly "mirror image" signal was observed in UVCD spectra of Eu(FOD) / *S*-1-phenylethanol and Eu(FOD) / *R*-1-phenylethanol ($c_{Eu(FOD)}$ = 50 µmol.dm^{-3}, $c_{S\text{-}PE/R\text{-}PE}$ = 500 µmol.dm^{-3}) solutions in n-hexane within 225 – 345 nm (figure 10). Next, a titration experiment of Eu(FOD) / *R*-PE solution was performed.

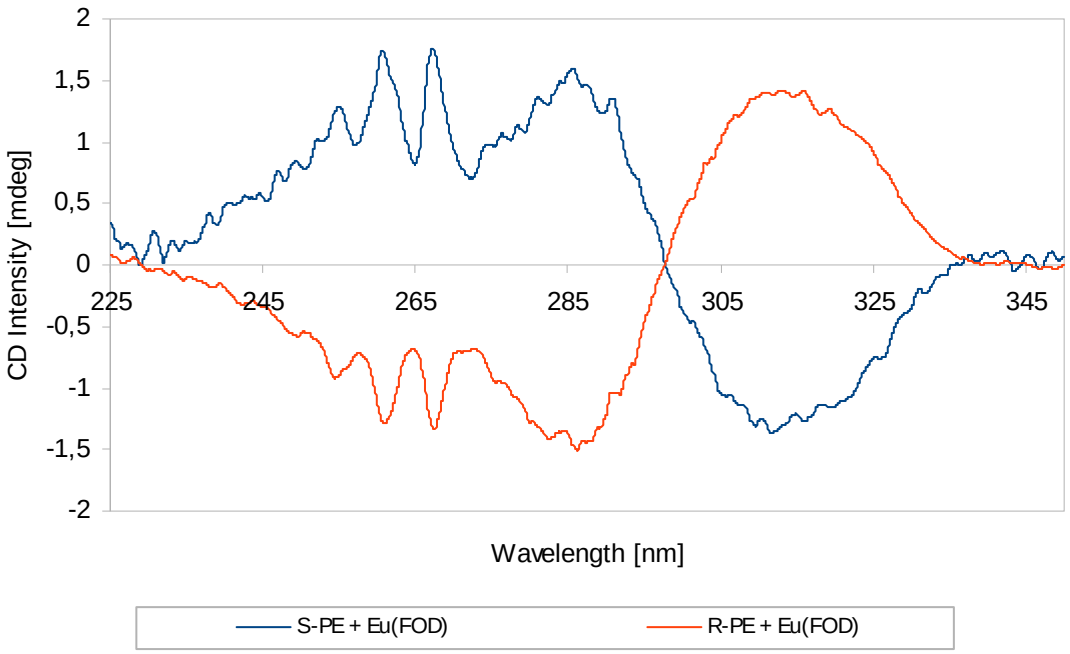

Figure 10. UVCD spectra of solutions containing Eu(FOD) and both (R-) and (S-) enantiomers of 1-phenylethanol in n-hexane: *Samples containing 50µM Eu(FOD) and (S-) and (R-) enantiomer of PE (500 µmol.dm^{-3}) both induced a strong mirror UVCD signal in the wavelength range of 225 – 350 nm.*

Samples of 50µM Eu(FOD) and 25 – 600µM *R*-PE in n-hexane were prepared so that the ratio of *lanthanide complex / chiral alcohol* was 1:0.5, 1:1, 1:1.5, 1:2, 1:2.5, 1:3, 1:3.5, 1:4, 1:5, 1:7, 1:10 and 1:12 (figure 11, part A; page 30). Several peaks were

observed. UVCD intensity of three peaks within 250 – 270 nm corresponding to *R*-PE showed a linear dependence on *R*-PE concentration in the sample. Since a couplet (two close peaks of opposite sign, in this case „-/+“ at ~285/315 nm) was not present in pure Eu(FOD) nor *R*-PE, its presence is likely to be induced by their complexation.

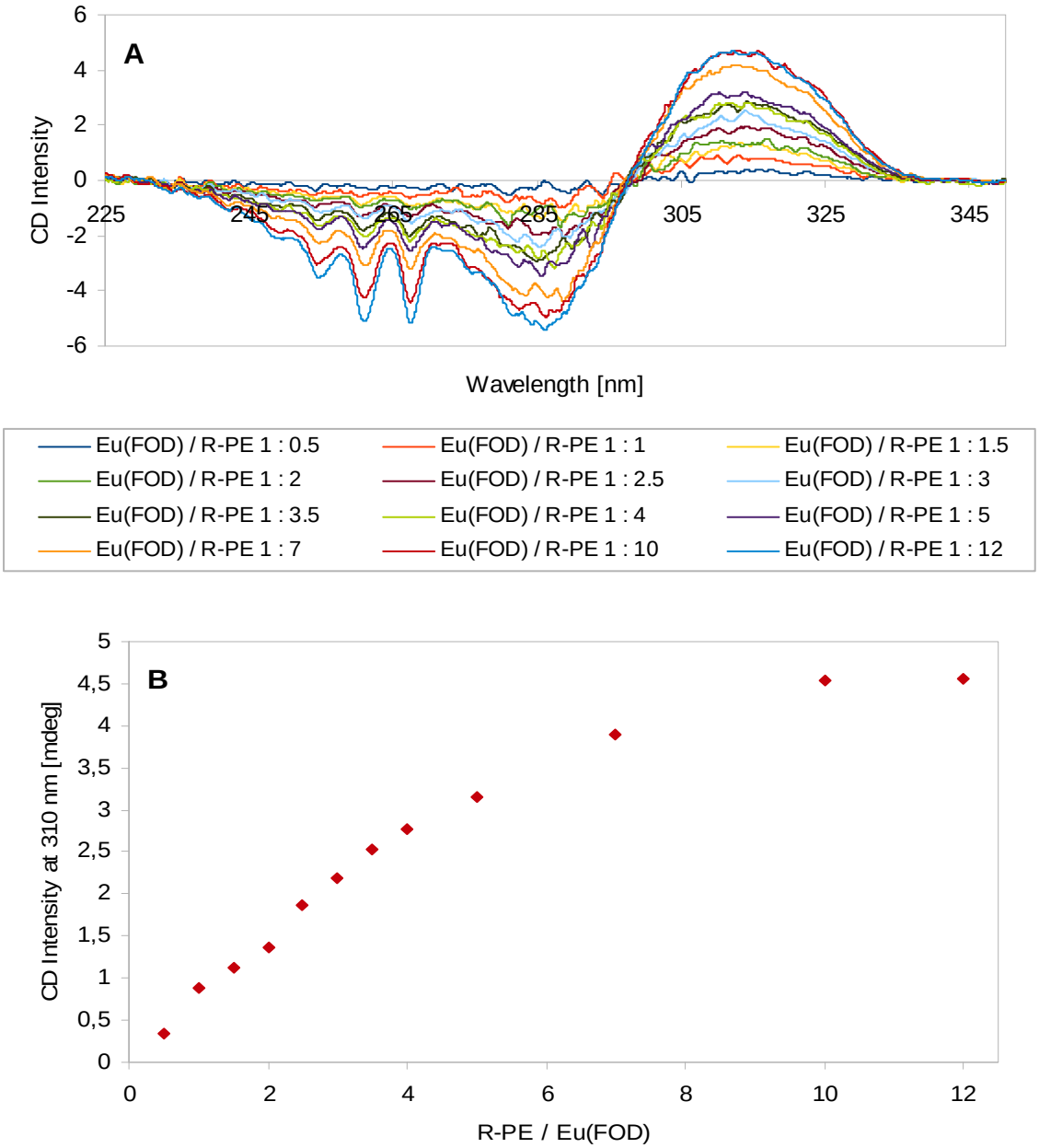

Figure 11. UVCD spectra of Eu(FOD) / R-PE mixtures in n-hexane. UVCD intensity at 310 nm is plotted as a function of the η: A: *Range of 225 – 350 nm for samples containing different concentration ratios of Eu(FOD) and R-1-phenylethanol in n-hexane.* ***B:*** *The intensity at 310 nm as dependent on the concentration ratio of R-PE / Eu(FOD). The curve saturates at* η *= 9:1, suggesting that 9 molecules of R-PE can bind to Eu(FOD) molecule.*

Maximum intensity at 310 nm (the amplitude of positive couplet peak) was plotted against **η** in Figure 11, part B (page 30). The intensity saturates at *R*-PE / Eu(FOD) ~ 9:1, suggesting that about 9 molecules of *R*-PE can interact with one Eu(FOD) molecule. Next, a similar plot showing the dependence of UVCD intensity at 287 nm (the amplitude of negative couplet peak) was created for lower *S*-PE / Eu(FOD) ratios (Figure 12). A very approximate sigmoid dependence was observed, and these data were used for the determination of the stability constant of 1:1 complex.

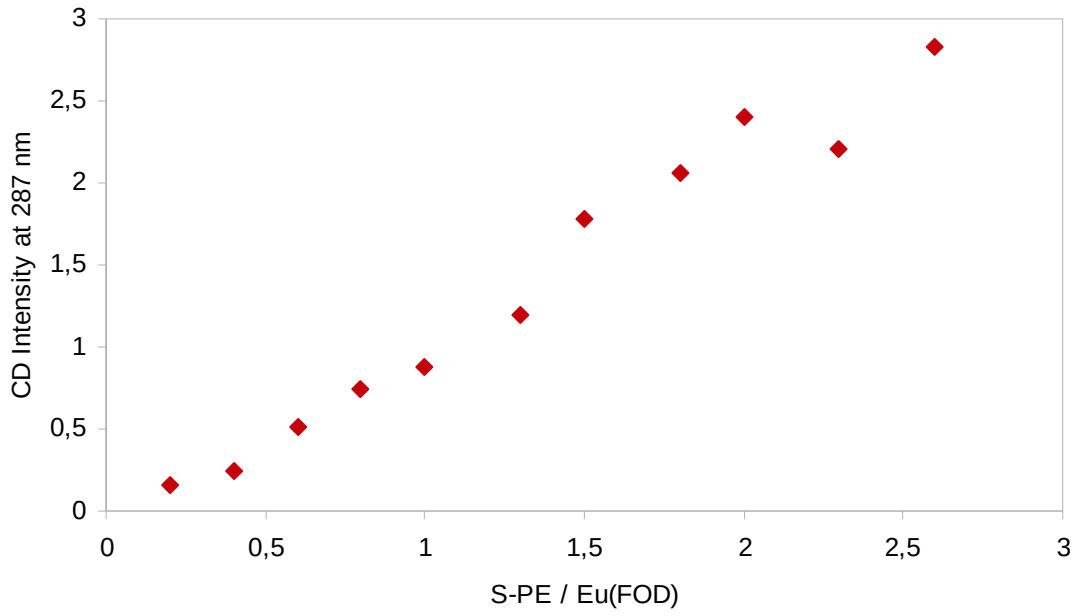

Figure 12. UVCD intensity at 287 nm plotted over S-1-phenylethanol / Eu(FOD: *UVCD intensity at 287 nm was plotted as a function of S-PE / Eu(FOD) concentration ratio for lower concentration ratios,* ***η*** *= 0.2:1 – 2.6:1.*

Forming of a 1:1 complex can be described by equation 19a. Stability constant *K* for 1:1 complex is then represented by equation 19b. We can relate UVCD intensity at 287 nm *CD* to the concentration of the complex formed *[COMPLEX]* according to the equation 19c. CD_S corresponds to the saturated UVCD intensity at 287 nm at the constant Eu(FOD) concentration.

$$PE + Eu(FOD) \leftrightarrow COMPLEX \qquad [19a]$$

$$K = \frac{[COMPLEX]}{([PE]_0 - [COMPLEX]).([Eu(FOD)]_0 - [COMPLEX])} \qquad [19b]$$

$$CD \approx \frac{[COMPLEX]CD_S}{[Eu(FOD)]_0} \qquad [19c]$$

[19d]

$$CD = \frac{[Eu(FOD)]_0 + [PE]_0 + \frac{1}{K} - \sqrt{([Eu(FOD)]_0 + [PE]_0 + \frac{1}{K})^2 - 4[Eu(FOD)]_0[PE]_0}}{2\frac{[Eu(FOD)]_0}{CD_S}}$$

Substituting eq. 19b to eq. 19c, we can derive eq. 19d. From the measured *CD*, $[Eu(FOD)]_0$ and $[PE]_0$ in eq. 19d, we determined the stability constant *K* for 1:1 complex with a non-linear least square fit. Then the stability constant for the PE / Eu(FOD) complex for **η** = 1:1 was determined as $K = 7.10^3$ $mol^{-1}.dm^3$. The theoretical dependence of the complex concentration (proportional to the UVCD signal) on the PE / Eu(FOD) ratio is plotted in Figure 13. It is in a good agreement with the experimental titration curves (see Figure 11, part B; page 30). For example, the complex concentrations starts to "saturate" at the PE / Eu(FOD) ratio of about 9:1.

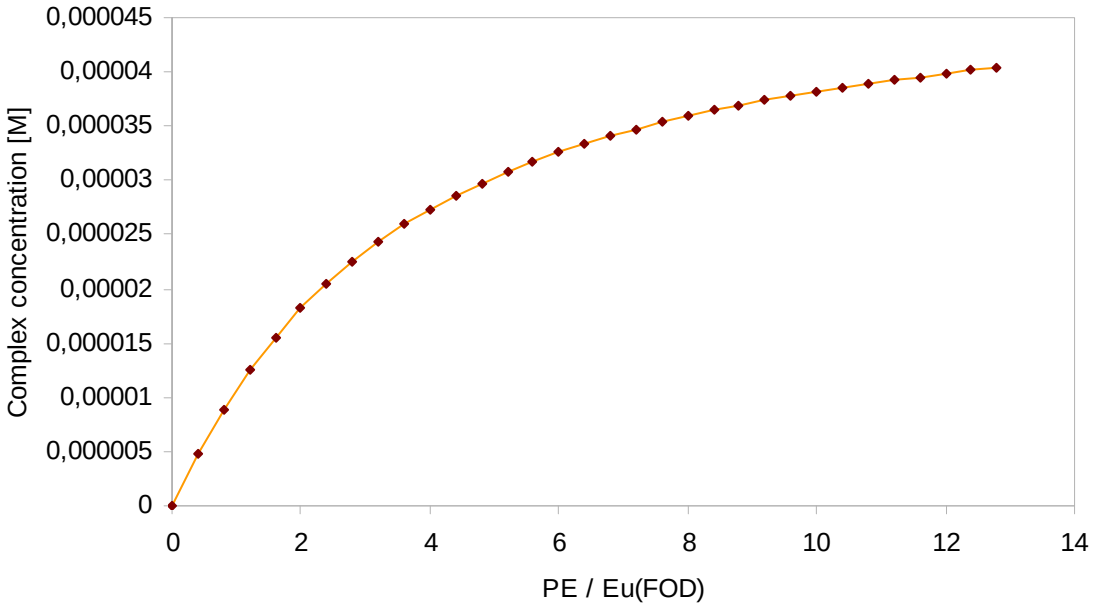

Figure 13. Calculated dependence of the complex concentration on the PE / Eu(FOD) ratio: *The curve seems to slowly saturate at the* **η** *≈ 9:1, which is in a good agreement with experimental results.*

4.2.1. Factor Analysis of Circular Dichroism Data

Factor analysis (FA) is a statistical method that can reduce experimental spectral data sets into fewer so called factors - subspectra, without a significant loss of information. It is often applied to Raman spectra analysis.[54, 55] Singular value decomposition (SVD) algorithm was used. The data (*N* spectra) are reduced to a sum of orthonormal subspectra (factors) multiplied by its scores (coefficients) and statistical weight (see Figure 14). When the dimension (*M*, number of the factors) is reduced, the sum gives a good approximation to the original spectra. We can then deduce that the number of the subspectra reflects the number of major species present in the sample.

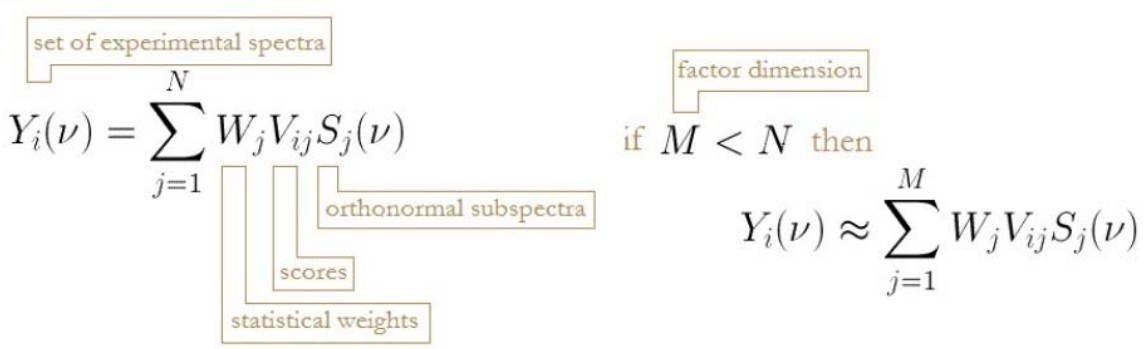

Figure 14. Factor Analysis by the Singular Value Decomposition: *The main idea is to reduce set of experimental spectra to fewer orthonormal subspectra, multiplied by its scores and statistical weights.*

FA was used to analyze UVCD data. The results can be seen in Figure 15 (page 34). The spectra of samples containg Eu(FOD) and *R*-1-phenylethanol in different concentration ratios (from 1:1 up to 1:12) were reduced to five subspectra (S1 – S5), but only two (S1 and S2) were determined as significant.

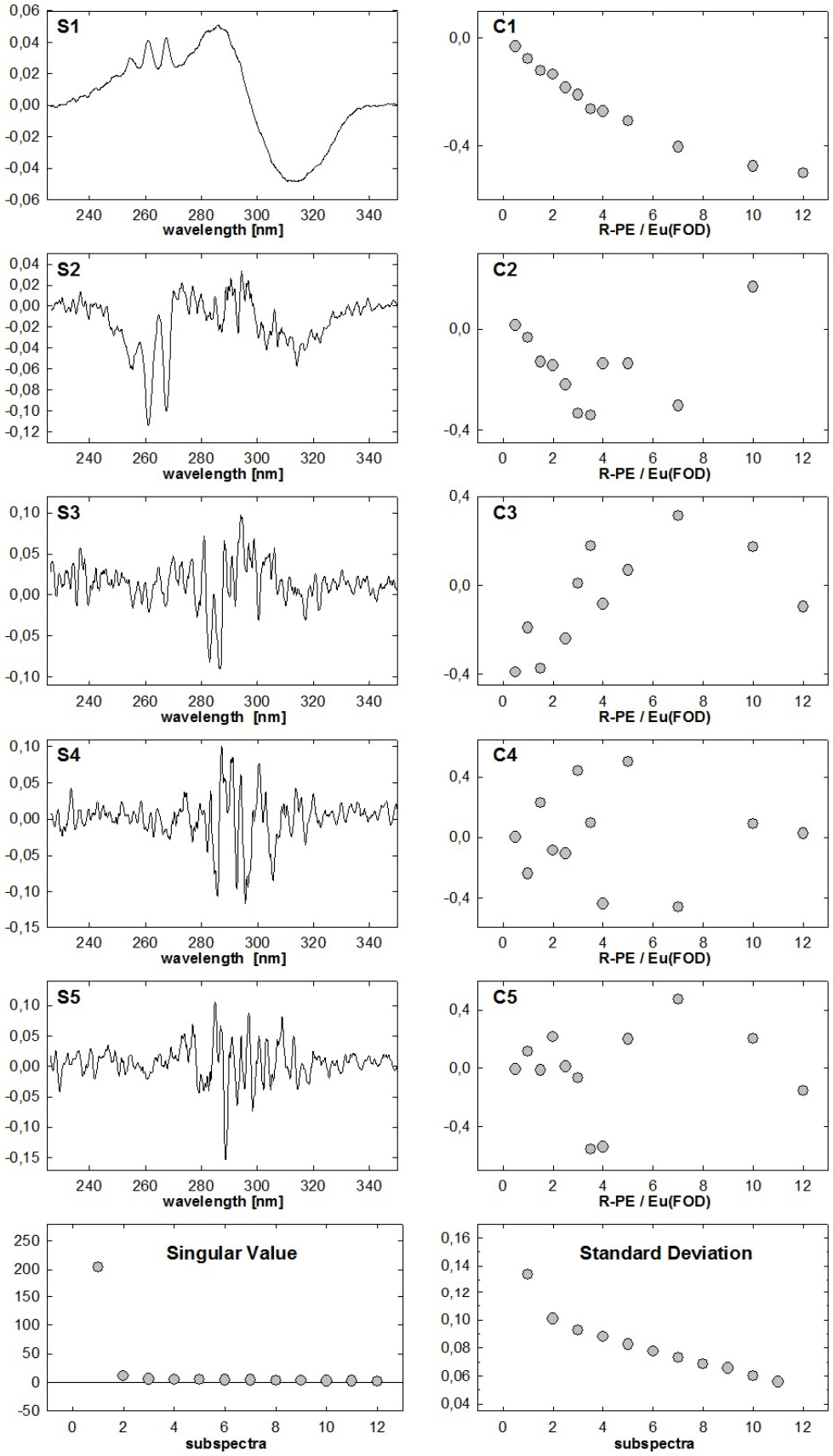

Figure 15. Factor Analysis for the UVCD titration experiment: *Left: the subspectra; right: the expansion coefficients; bottom two panels: singular values (weights), and standard deviations.*

4.3. Raman Scattering and Raman Optical Activity of Eu(FOD) / 1-Phenylethanol

Another method used for studying optically active molecules is Raman optical activity (ROA). Since a vibrational spectrum usually contains many bands, ROA can provide much more information than UVCD. The Raman effect occurs with visible exciting light, which is a convenience against the vibrational circular dichroism (VCD).[56] However, since the differential intensity is very small, long measurement times and high sample concentrations are needed. This problem can be overcome by induced resonance. In this case, a high-spin Eu^{3+} ion provides electronic transition ($^5F_0 \rightarrow {}^5D_0$) corresponding to the wavelength of 532 nm typically used in ROA experiments. Therefore the sensitivity of the measurement is enhanced.[57]

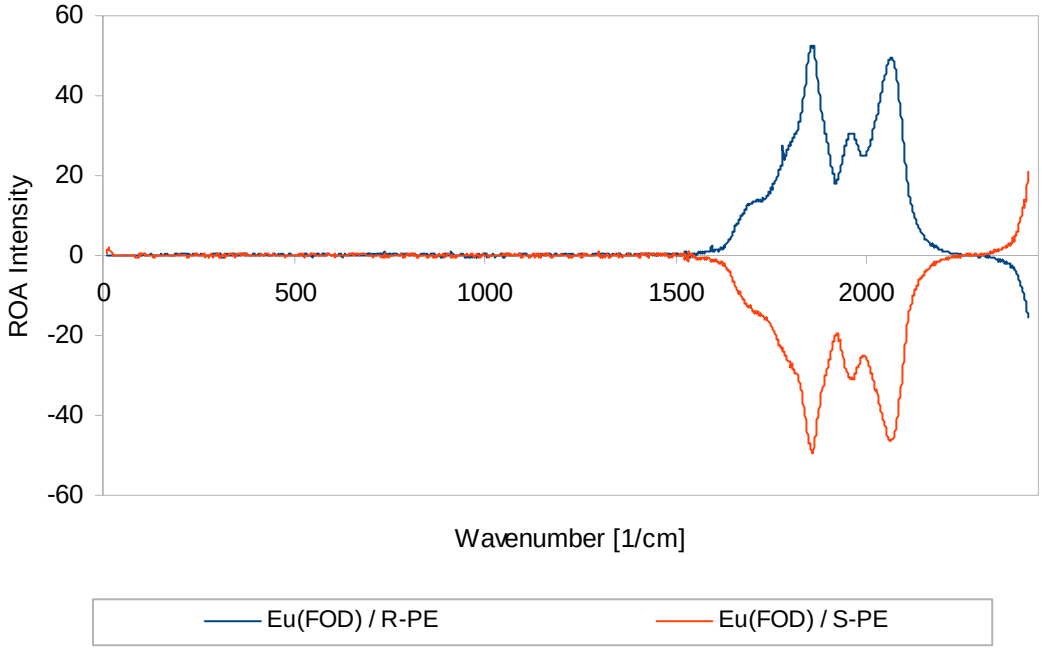

Figure 16. Raman Optical Activity of Eu(FOD) / 1-Phenylethanol: *Samples containing both enantiomers of 10mM 1-phenylethanol and 1mM Eu(FOD) in n-hexane revealed strong opposite ROA signals between 1500 – 2300 cm^{-1}.*

We were able to use this resonance phenomenon for collection of Raman Scattering and ROA spectra of samples containing constant Eu(FOD) concentration (1 $mmol.dm^{-3}$) and both *(R)*- and *(S)*- enantiomers of 1-phenylethanol in various concentrations (giving

ratios from 1:0.5 to 1:15). Upon complexation with Eu(FOD), both enantiomers of 1-phenylethanol gave a strong „mirror image“ ROA signal (Figure 16; page 35).

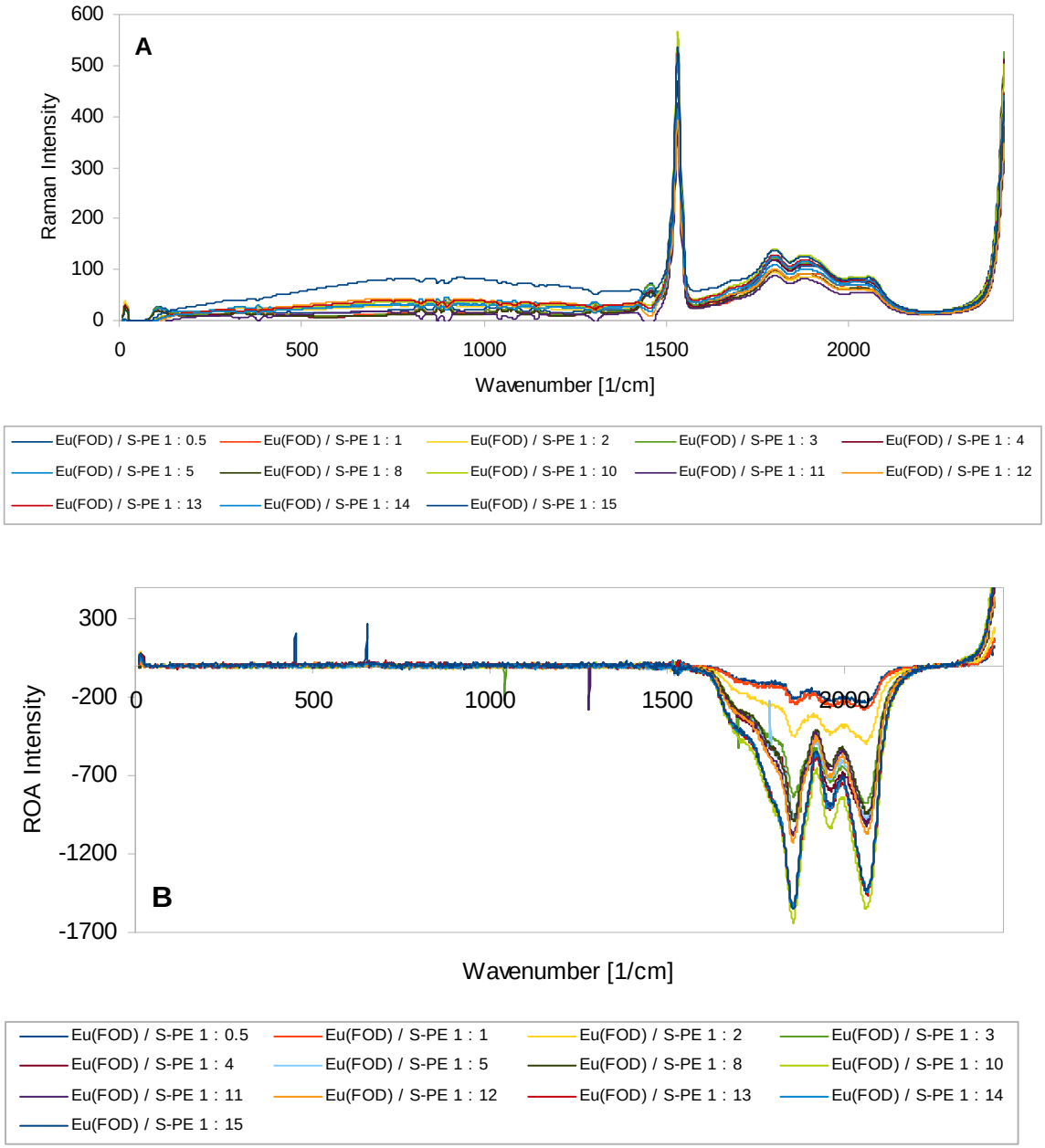

Figure 17. Raman Scattering and Raman Optical Activity spectra of Eu(FOD) / S-PE complex: A: *Raman scattering spectra of Eu(FOD) / S-PE mixtures of different* ***η*** *(Eu(FOD) concentration held constant at 1mM, S-PE concentration ranging depending on* ***η****) in n-hexane.* ***B:*** *ROA spectra of Eu(FOD) / S-PE mixtures of different* ***η*** *(Eu(FOD) concentration held constant at 1mM, S-PE concentration ranging depending on* ***η****) in n-hexane.*

Titration experiment of Eu(FOD) / *S*-PE was performed and Raman Scattering and ROA spectra were collected (Figure 17, part A and B; page 36). Eu(FOD) concentration in n-hexane was held constant at 1mM, *S*-PE concentration was ranging depending on the desired **η**. Strong ROA and Raman signals were observed for wavenumbers 1600 cm^{-1} and greater. These signals correspond to electronic transitions of Eu^{3+} ion ($^7F_0 \rightarrow {}^7F_4$ at 2439 cm^{-1} and $^7F_0 \rightarrow {}^7F_3$ within 2200-1600 cm^{-1}).

ROA intensity at 1863 cm^{-1} (expressed as number of electrons e^- recorded by the CCD detector) was plotted against **η** (Figure 18, part A; page 38). Even though the intensity of ROA signal at 1863 cm^{-1} increased with higher *S*-PE / Eu(FOD) concentration ratio, this increase was erratic. Better results were obtained when circular intensity difference (CID) was plotted as a function of **η** (Figure 18, part B; page 38). CID was calculated as a ratio of Raman intensity I_{Raman} to ROA intensity I_{ROA} at 1863 cm^{-1} (eq. 20). CID at 1863 cm^{-1} saturates at **η** = 4:1.

$$CID = \frac{I_{Raman}}{I_{ROA}} \text{ at } 1863 \text{ cm}^{-1} \qquad [20]$$

4.3.1. Factor Analysis of Raman Optical Activity

Factor Analysis with the use of SVD algorithm was used to treat ROA spectral data. Original sets of spectra were reduced to subspectra with corresponding statistical weights and coefficients. The output of this analysis for experimental ROA spectra can be seen in Figure 19 (page 39). The spectra of samples containg Eu(FOD) and *S*-1-phenylethanol in different **η** (from 1:1 up to 1:16) were reduced to five subspectra (S1 – S5), but only three (S1, S2 and S3) were determined as significant.

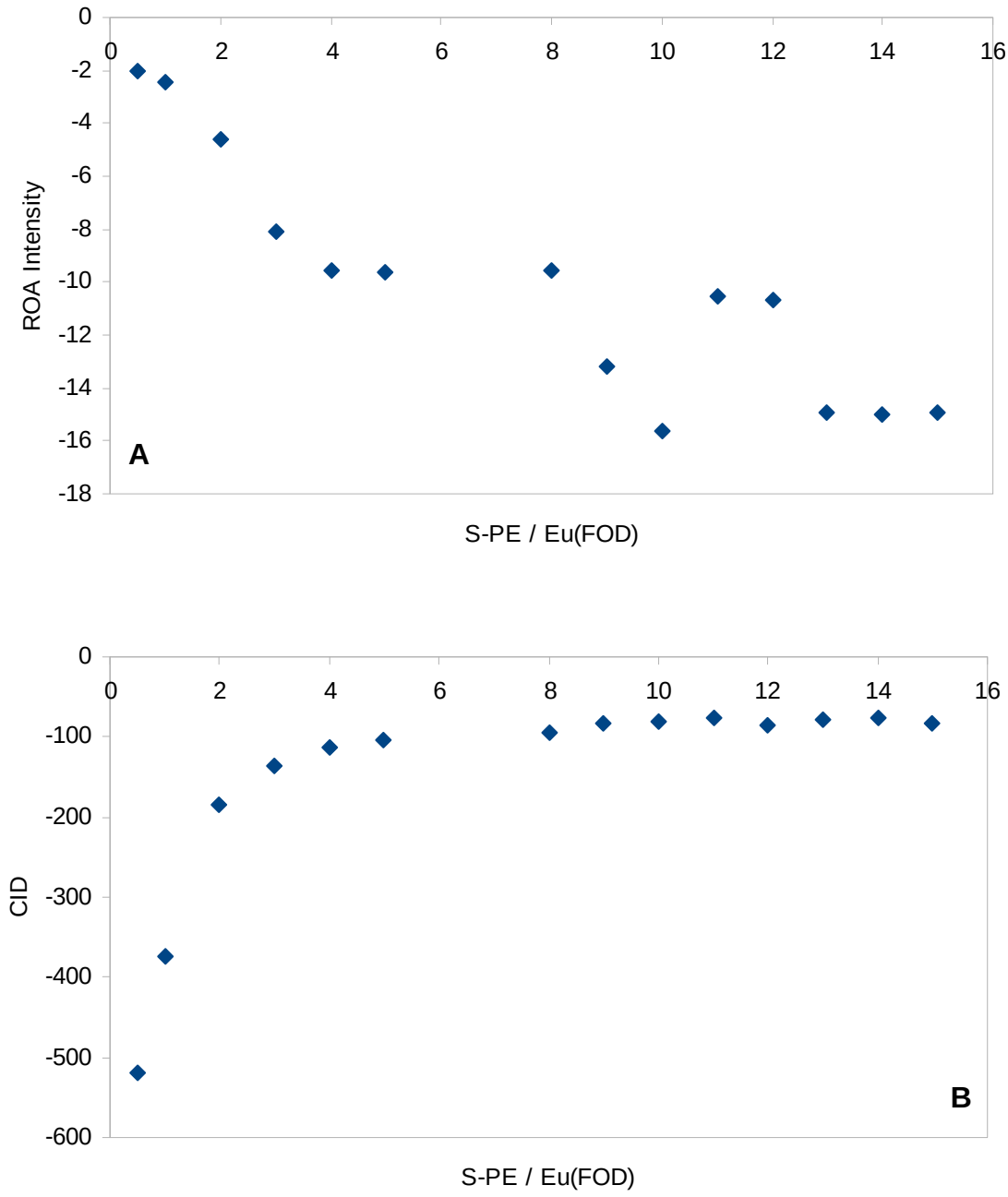

Figure 18. Plots of CID and ROA intensity against the Eu(FOD) / S-PE concentration ratio: A: *ROA intensity at 1863 cm^{-1} plotted as a function of* ***η****.* ***B:*** *Circular Intensity Difference at 1863 cm^{-1} plotted as a function of* ***η****. The curve saturates at* ***η*** *= 4:1.*

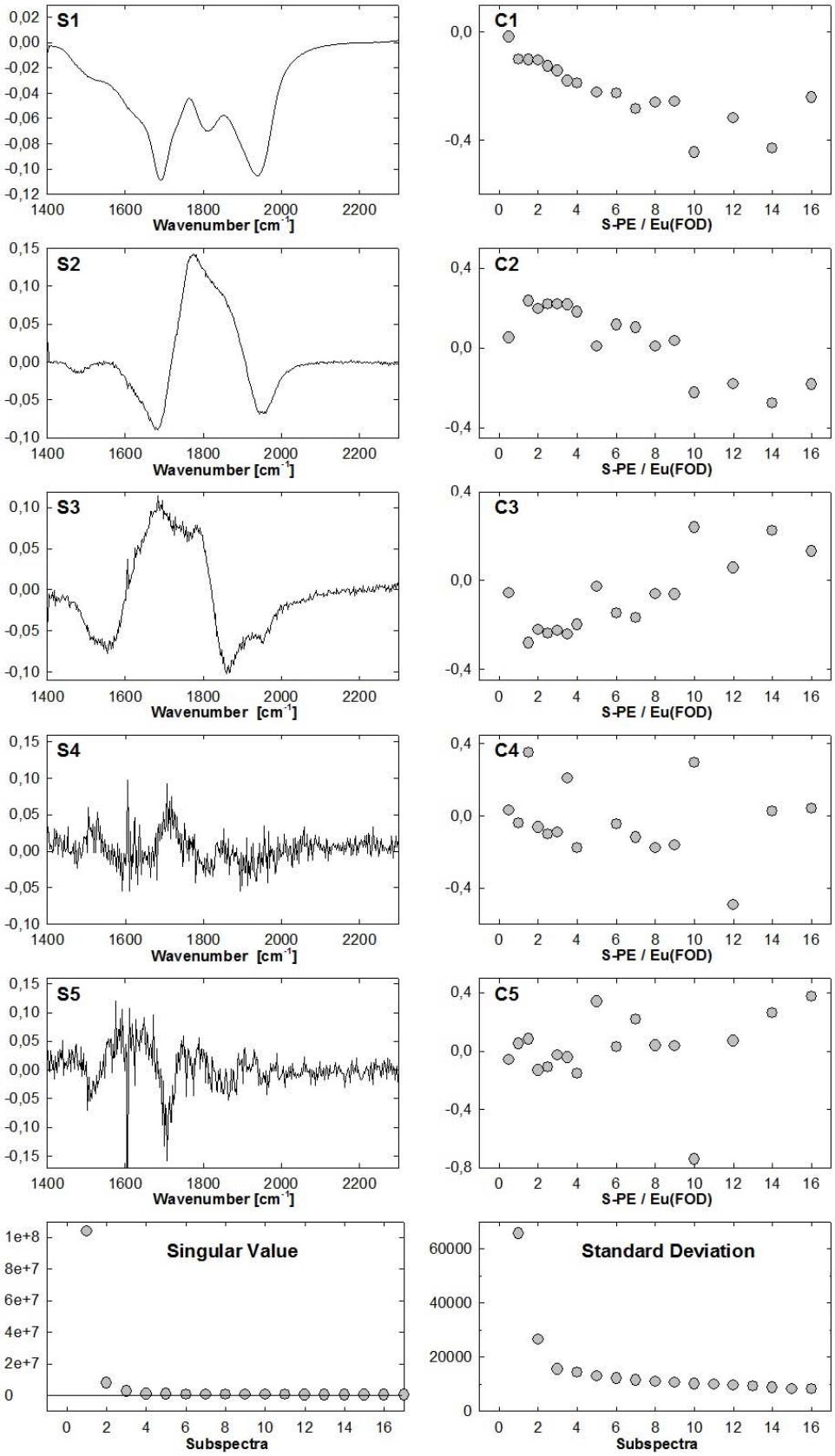

Figure 19. Factor analysis of data obtained by ROA titration experiment: *Left: the subspectra; right: the expansion coefficients; bottom two panels: singular values (weights), and standard deviations.*

4.4. Infrared Spectroscopy of Eu(FOD) / 1-Phenylethanol

Infrared spectroscopy analyzes an interaction of infrared light with a molecule by measuring the absorption, emission or reflection of IR electromagnetic radiation. The energy of this radiation is sufficient to cause vibrational (higher-energy near-IR), rotational-vibrational (mid-IR) and rotational (far-IR) changes.

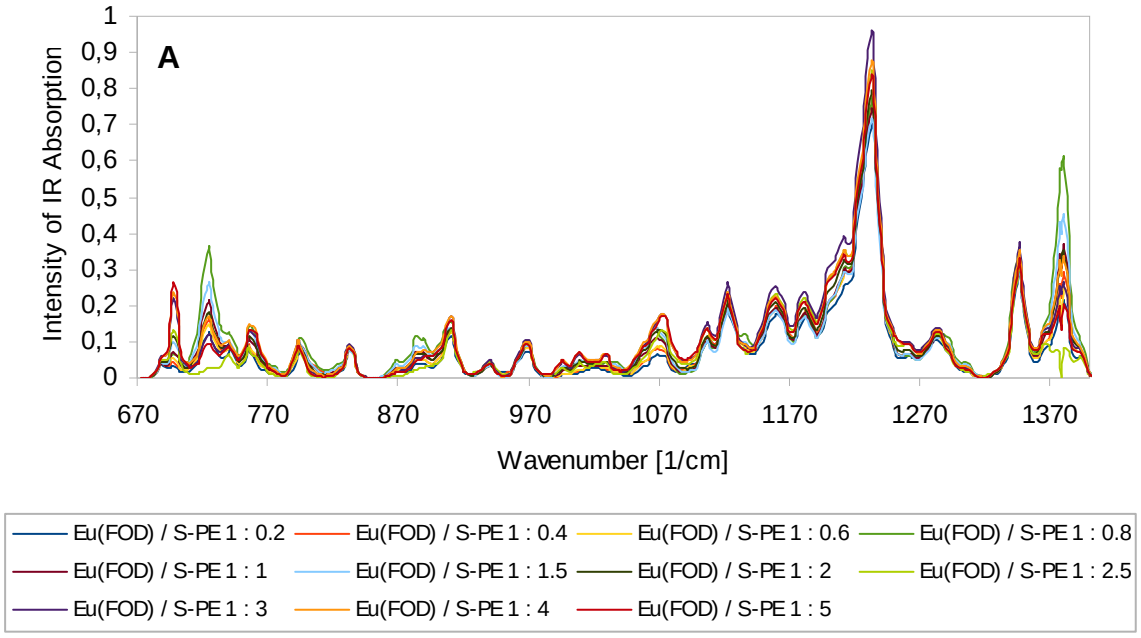

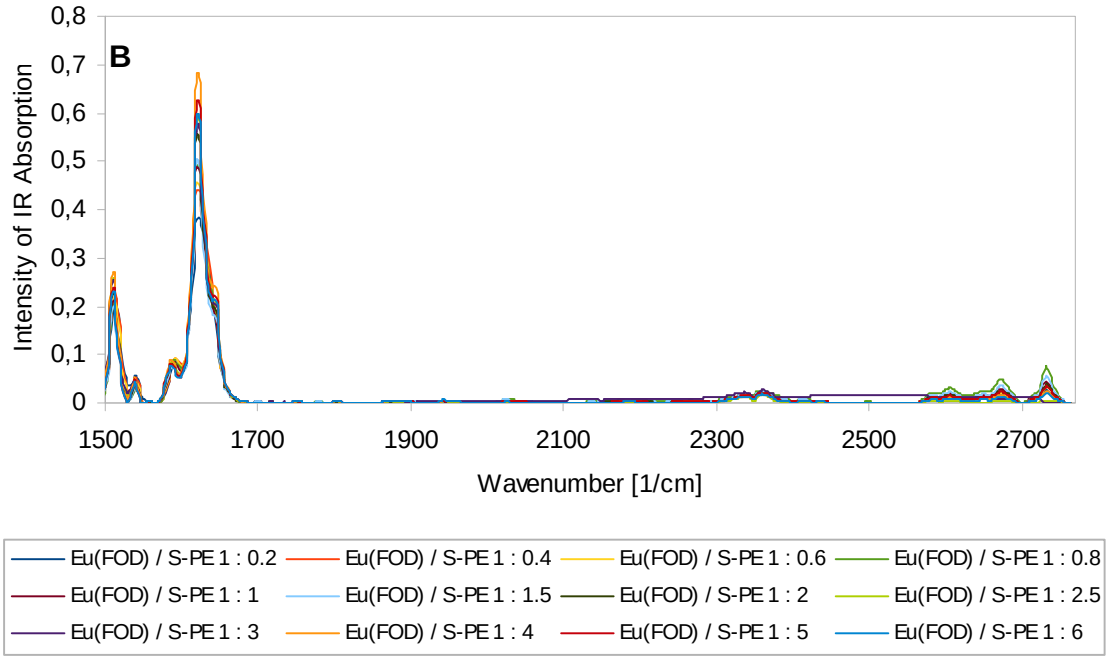

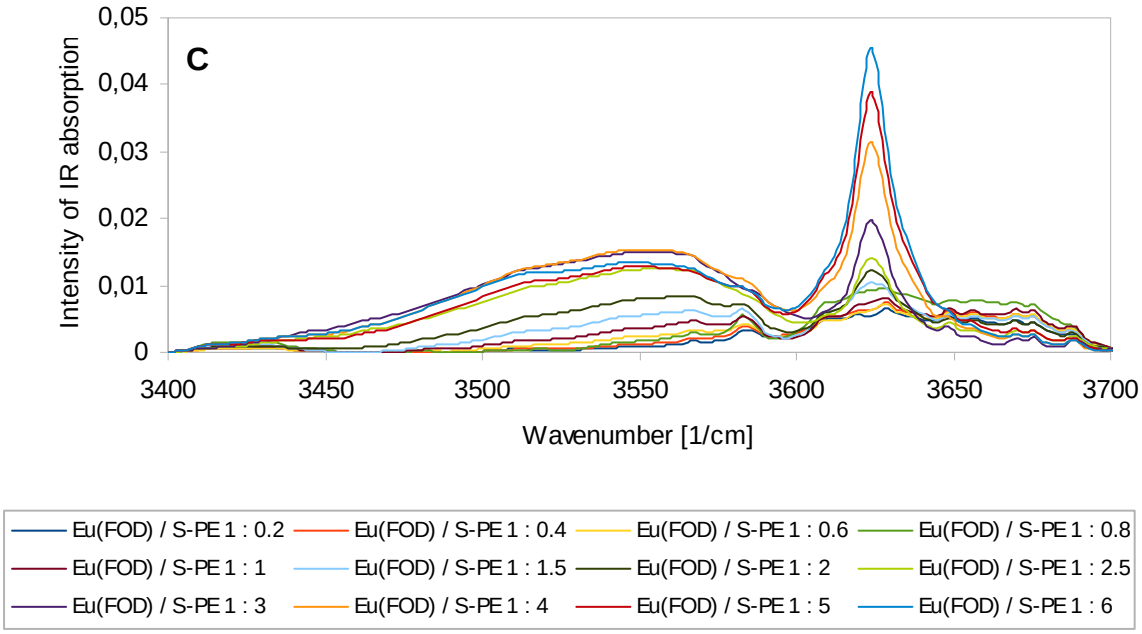

Figure 19. IR absorption spectra of Eu(FOD) / S-1-phenylethanol: A: *IR absorption spectra from* **η** *= 0.2:1 to* **η** *= 5:1 within 670 – 1400 cm^{-1}.* ***B:*** *IR absorption spectra from* **η** *= 0.2:1 to* **η** *= 6:1 within 1500 – 2750 cm^{-1}.* ***C:*** *IR absorption spectra of Eu(FOD) / S-PE solution in n-hexane from* **η** *= 0.2:1 to* **η** *= 6:1 within 3400 – 3700 cm^{-1}. Absorption bands corresponding to -OH group of PE and H-bond formation are visible.*

We measured absorption IR spectra of Eu(FOD) / PE mixtures. Collected IR spectra for this complex (12.5mM Eu(FOD), concentration of *S*-PE ranging depending on desired **η**) were divided into three regions – low-IR (Figure 19, part A), middle-IR (Figure 19, part B) and high-IR (Figure 19, part C). Even though several absorption bands were observed, dependence of their intensity on **η** was rather chaotic. IR absorption at 3623 cm^{-1} and below corresponds to vibrations of *-OH* group of 1-phenylethanol molecule with obvious H-bond formation between 3500 – 3600 cm^{-1} (Figure 19, part C). IR absorption in this region is stronger with increasing **η** suggesting stronger H-bond formation in concentrated PE solutions.

5. DISCUSSION

Many biologically relevant compounds such as proteins, nucleic acids, sugars, amino acids, hormones or pharmaceutical agents exhibit specific functionality depending on their chirality. Therefore chiral recognition of biological molecules is of a crucial importance. Chiral recognition is conventionally done by spectroscopic techniques sensitive to optical activity of the sample. However, in some cases these techniques do not offer desired results and must be refined. It was shown that chirality sensing of biological substrates via lanthanide coordination chemistry can be very beneficiary. However, further experiments are needed to fully understand the nature /of *lanthanide complex – chiral molecule* interaction.

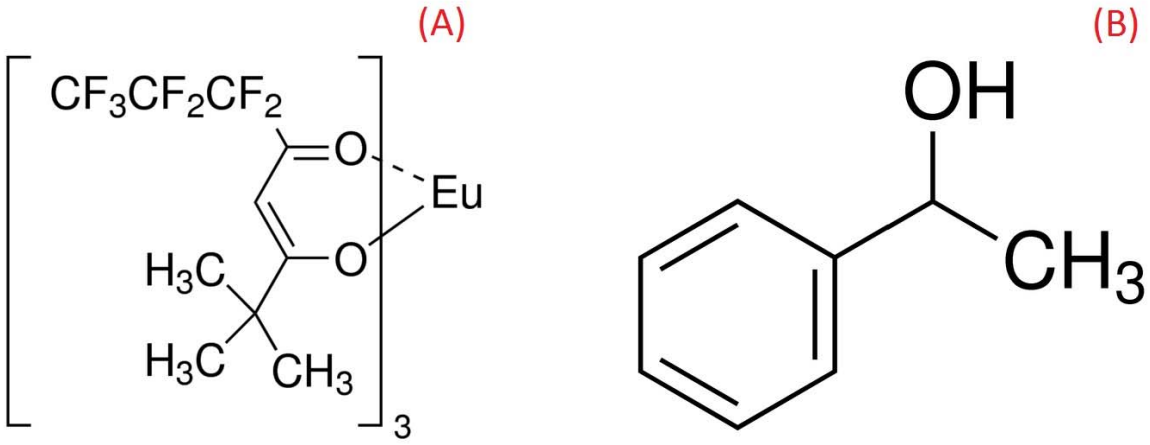

Figure 20. Chemical Structure of Eu(FOD) and PE: A: *A chemical structure of Eu(FOD) is shown. Three β-diketonate ligands are coordinated to* Eu^{3+} *ion. Fluorinated ligands promote anion coordination with lanthanide center and enhance the carrier activity.*[58] *However, if tris-(β-diketonate) ligands are used, aminoalcohols and amines are capable of forming Schiff bases with the coordinated ligands and therefore no structure – spectra correlation are possible.*[59, 60] *Therefore, we used a simple chiral alcohol 1-phenylethanol (**B**) as a substrate.*

We studied this interaction using a model system consisting of europium tris(6,6,7,7,8,8,8-heptafluoro-2,2-dimethyloctane-3,5-dione) with 1-phenylethanol (Figure 20). Several studies in which optical activity has been induced in achiral Eu^{3+} compounds through complexation with chiral substrates have been published.[61, 57] Since complexation of a chiral non-chromophoric substrate to Eu^{3+} complex can induce chirality detectable by

spectroscopic methods and therefore it can provide a means of spectroscopic chirality determination of substrates normally silent in spectra, further studies of such compounds are needed. We used several spectroscopic methods such as UV-Vis absorption spectroscopy, ultraviolet circular dichroism, Raman scattering and Raman optical activity, and infrared spectroscopy.

The results obtained by UV-Vis spectroscopy were inconclusive. Strong absorption band within 260 – 340 nm as the most promising signal was linearly dependent on the Eu(FOD) concentration. However, UV-Vis absorption bands of lanthanide ions due to transitions within *4f* levels are not much affected by changes in the environment of the ion. The absorption spectra thus cannot account for complex formation. Sometimes small red shifts and splitting of certain bands into several small maxima as well as variations of absorbance of individual peaks were observed. However, these changes are usually too small to be used to study the change in coordination environment of the central ion.[45]

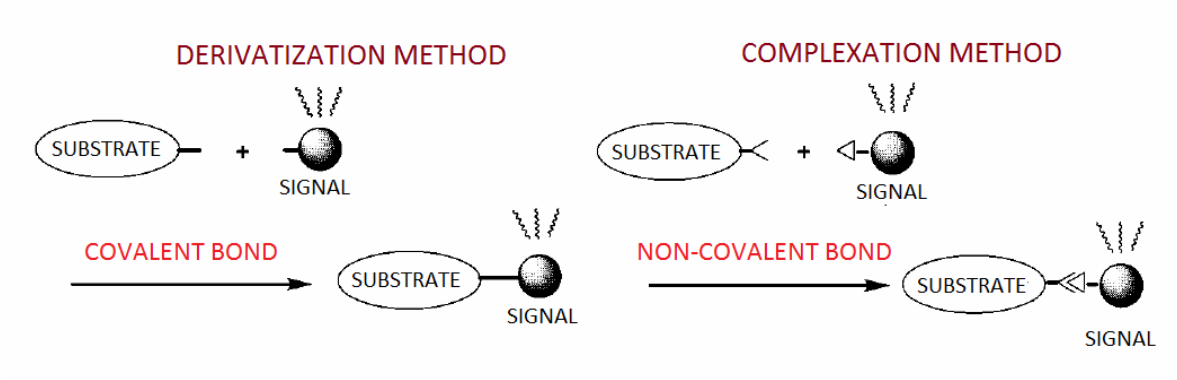

Figure 21. Comparison of derivatization and complexation method of chirality sensing:[62] *When a non-chromophoric substrate is examined by spectroscopic methods, a chromophore must be attached by derivatization or complexation. The derivatization requires bond formation between the substrate and a chromophore, while complexation method is based on a non-covalent interaction.*

Next, we used UVCD. UVCD is applicable only to molecules containing chromophore absorbing in UV or Vis spectral range. Even though this restriction limits the use of UVCD, non-chromophoric substrates can be examined if a chromophore is attached to the molecule by derivatization or complexation method (Figure 20). However, the derivatization requires bond formation between the chromophore and a substrate, and often a series of laborious procedures which include coupling reaction between the chromophore and the substrate is necessary. A purification is needed. Substrate recovery is also very

difficult. In the case of the complexation, substrate forms a donor-acceptor bond with a metal ion. Metal ion provides electronic transitions needed for UVCD measurement, while measured chirality is induced solely by a chiral molecule. No covalent bond formation between the two species or purification steps are needed. Substrate recovery is much easier than in the case of the derivatization. Therefore, the complexation method is often viewed as a better alternative.[/62/]

1-Phenylethanol contains an aromatic chromophore active in UVCD spectra within 240 – 275 nm. However, we studied the complex formation by examining the UVCD couplet within 270 – 335 nm induced by a complex formation between Eu(FOD) and PE. Eu(FOD) otherwise silent in UVCD spectra provides an electronic transition within this wavelength range, while the chirality is induced by PE. The titration experiments showed, that this signal saturates at $\boldsymbol{\eta}$ = 9:1 suggesting that up to 9 molecules can participate in complex formation.

We hypothesize that as the concentration of PE in the sample increases, different complex species are present in the solution. At low PE concentrations, 1 or 2 PE molecules can bind to the Eu(FOD) molecule forming highly coordinated complex. At higher PE concentrations, 1 or several tris-β-diketonate ligands in Eu^{3+} coordination sphere are substituted by PE molecules. We assume that the complex formed at $\boldsymbol{\eta}$ = 9:1 consists of 9 molecules of PE totally substituting the *β*-diketonate ligands. Using the dependence of UVCD signal intensity at 287 nm plotted against the $\boldsymbol{\eta}$ for lower concentration ratios (Figure 12; page 31), approximate value of stability constant for $\boldsymbol{\eta}$ = 1:1 was determined to be $K = 7.10^3$ $mol^{-1}.dm^3$.

Next, a Raman optical activity titration experiment was performed. This technique can reveal a lot of information about configuration of chiral compound, but the differential intensity is very small and therefore long ROA accumulation times as well as high sample concentrations are needed. However, this can be overcome by an induced resonance (Figure 22, page 45). About a 10^2-fold ROA signal enhancement if compared to non-resonant vibrational ROA was observed. IRROA is for example observed when a chiral substrate couples with Eu^{3+} complex in solution. Eu^{3+} ion provides electronic transitions in resonance with the laser excitation wavelength what leads to the large polarizability and consequent intense Raman signal.[/57/]

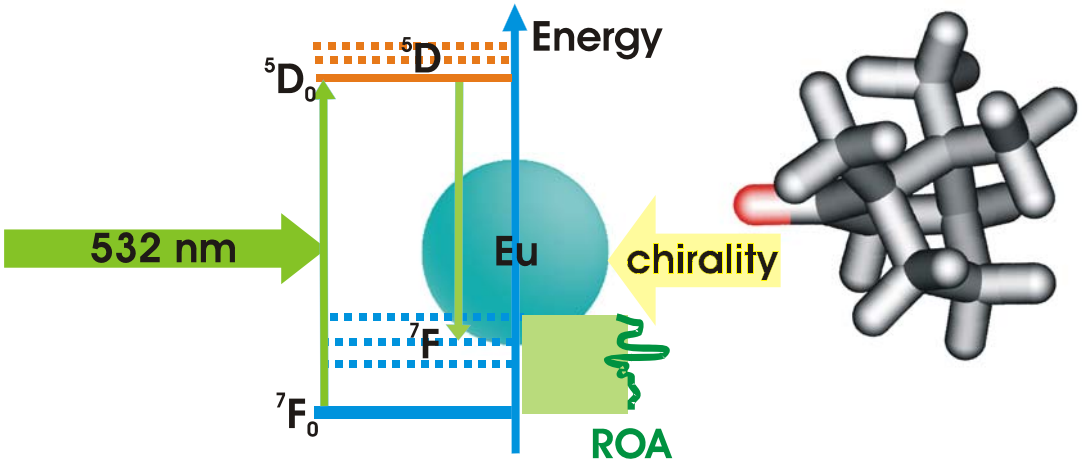

Figure 21. Induced resonance Raman optical activity:[57] *High spin Eu^{3+} ion provides an electronic transition $^7F_0 \rightarrow {}^5D_0$ close in energy to the laser excitation wavelength 532 nm. When a complex of Eu^{3+} coupled with a chiral compound is irradiated by a laser light of 532 nm, Raman signal is greatly enhanced while the chirality measured is induced by a chiral molecule. This method therefore combines the sensitivity od ROA for the structure with the enhanced sensitivity of resonant Raman spectroscopy.*

We were able to use this resonance phenomenon in Raman Scattering for ROA spectra collection. Both circular intensity difference and Raman optical activity signal intensity at 1863 cm^{-1} seemed to saturate at **η** = 4:1 (see section 4.3.). When compared to results obtained by UVCD (see section 4.2.), CID saturates at lower PE / Eu(FOD) concentration ratios (**η** = 9:1 for UVCD vs. **η** = 4:1 for ROA). Since these two techniques are of different physical basis, their sensitivity towards individual Eu(FOD) / PE adducts present in the solution can be different.

Factor analysis was used to treat experimental spectra obtained by ultraviolet circular dichroism and Raman optical activity. The spectra can be reduced to several subspectra. The number of significant subspectra can be linked to the number of active species in the solution. Only 2 subspectra were considered to be significant when factor analysis was employed to study UVCD spectra, while factor analysis of ROA spectra gave 3 significant subspectra. We hypothesize that the significant subspectra correspond to the Eu(FOD) / PE adducts of different stoichiometry.

Infrared spectroscopy was also used to study this *lanthanide complex – chiral alcohol* interaction, but the results were inconclusive. Even though a number of IR absorption bands was observed, their intensity plotted over **η** was purely erratic (see section 4.4.).

Therefore, we can conclude that only Raman optical activity and ultraviolet circular dichroism are suitable to study the interaction of Eu^{3+} complex with chiral 1-phenylethanol. Thanks to the complexation of PE with Eu(FOD), new absorption bands arise in UVCD spectra as a result of Eu^{3+} electronic transitions coupled with chirality induced by a chiral molecule coordinated to Eu(FOD). Complexation of a chiral substrate to Eu^{3+} complex can be convenient also in the Raman optical activity. Since electronic transitions of Eu^{3+} ion provide basis for resonant Raman signal enhancement, the sensitivity of ROA measurement is enhanced. A complexation method with the use of Eu^{3+} complexes can thus be used to improve the chirality sensing of chiral molecules by UVCD and ROA techniques. Further studies with computational analysis are needed to better understand the nature of this interaction.

6. CONCLUSION

The aim of this work was to study an interaction of europium tris(6,6,7,7,8,8,8-heptafluoro-2,2-dimethyloctane-3,5-dione) with a chiral organic alcohol 1-phenylethanol using spectroscopic methods such as UV-Vis absorption spectroscopy, ultraviolet circular dichroism, Raman scattering and Raman optical activity, and infrared spectroscopy. The results we have obtained can be summarized as follows:

- Only ultraviolet circular dichroism and Raman optical activity were sensitive enough to the complexation.

- Upon complexation of PE to Eu(FOD), strong couplet UVCD signal within 270 – 335 nm was induced. The intensity at 310 nm plotted as a function of **η** (**η** = PE / Eu(FOD) concentration ratio) saturates at **η** = 9:1 suggesting that totally 9 molecules of PE can interact with Eu^{3+} ion.

- Similar curves for lower **η** showed nearly sigmoidal dependence for **η** = 1:1 complex. These data were used to determine stability constant of this complex $K = 7.10^3$ $mol^{-1}.dm^3$.

- Raman optical activity is a powerful method for studies of biologically relevant compounds. The need for a high sample concentration and long measurement times can be overcome by a complexation of a chiral molecule to Eu^{3+} complex that provides strong induced resonance and therefore a significant Raman signal enhancement.

- Both the ROA intensity at 1863 cm^{-1} and CID plotted against **η** seemed to saturate at **η** = 4:1.

- In the factor analysis, several active species were identified in the UVCD (2 active species) and ROA (3 active species) spectra. Factor analysis proved to be a valuable tool in UVCD and ROA spectral interpretation.

- Since the complexation of 1-phenylthanol to Eu(FOD) induces the enhanced ROA signal and provides a strong UVCD signal, this method can be useful for chiral recognition of several classes of chiral substrates. In the future, such chirality detection should be further refined by rational design of the ligands and experimental conditions.

REFERENCES

/01/ Fišer, J. in *Úvod do molekulové symetrie*; Státní pedagogické nakladatelství Praha; **1976**

/02/ *Picture taken from:* http://chemwiki.ucdavis.edu/Organic_Chemistry/Chirality/Chirality_and_Stereoisomers; 2014/08/02 at 8.56 pm.

/03/ McMurry, J. E. in *Organic Chemistry 8th Ed.*; Brooks/Cole; **2010**

/04/ Wigner, E: *Z. Physik* **1927**; 43; 624

/05/ Quack, M.; Stohner, J.: *Chirality* **2001**; 13; 745

/06/ Hegstrom, R. A.; Rein, D. W.; Sandars, P. G. H.: *Chem. Phys.* **1980**; 73; 2329

/07/ Mason, S. F.; Tranter, G. E.: *Mol. Phys.* **1984**; 53; 1091

/08/ Bakasov, A.; Ha, T. K.; Quack, M.: *J. Chem. Phys.* **1998**; 109; 7263

/09/ Barron, L. D.; Buckingham, A. D.: *Chem. Phys. Lett.* **2010**; 492; 199

/10/ Buckingham, A. D.: *Adv. Chem. Phys.* **1967**; 12; 107

/11/ Averill, B.; Eldredge, P. in *General Chemistry: Principles, Patterns, and Applications*; online version at http://catalog.flatworldknowledge.com/bookhub/4309?e=averill_1.0-ch24_s02#averill_1.0-ch02; Flat World Education, Inc.; **2014**

/12/ *Picture taken from:* http://www.rowland.harvard.edu/rjf/fischer/background.php; 2014/08/02 at 9.31 pm.

/13/ Ohmatsu, K.; Ito, M.; Kunieda, T.; Ooi, T.: *Nat. Chem.* **2012**; 4; 473

/14/ Wickremsinhe, E. R.; Tian, Y.; Ruterbories, K. J.; Verburg, E. M.; Weerakkody, G. J.; Kurihara, A.; Faris, N. A.: *Drug Metab. Dispos.* **2007**; 35; 917

/15/ Stephens, T. D.; Bunde, C. J. W.; Fillmore, B. J.: *Biochem. Pharm.* **2000**; 59; 1489

/16/ Atkins, P.; Paula, J. D. in *Physical Chemistry 8th Ed.*; W. H. Freeman and Company; **2006**

/17/ Yang, J. T.; Doty, P: *J. Am. Chem. Soc.* **1957**; 79; 761

/18/ Moffitt, W.; Yang, J. T.: *Proc. Natl. Acad. Sci. USA* **1956**; 42; 596

/19/ Berova, N.; Nakanishi, K.; Woody, R. in *Circular Dichroism: principles and applications 2nd Ed.*; Wiley-VCH, Inc.; **2000**

/20/ Kodíček, M.; Karpenko, V. in *Biofysikální Chemie 2nd Ed.*; Academia; **2000**

/21/ *Picture taken from:* http://www.ruppweb.org/cd/cdtutorial.htm; 2014/08/02 at 10.22 am.

/22/ *Picture taken from:* http://www.proteinchemist.com/cd/cdspec.html; 2014/08/02 at 2.56 pm.

/23/ Sreerama, N.; Woody, R. W.: *Anal. Biochem.* **2000**; 287; 252

/24/ Lobley, A.; Whitmore, L.; Wallace, B. A.: *Bioinformatics* **2002**; 18; 211

/25/ Whitmore, L.; Wallace, B. A.: *Nucl. Acids Res.* **2004**; 32; 668

/26/ Holzwarth, G.; Hsu, E. C.; Mosher, H. S.; Faulkner, T. R.; Moscowitz, A. J.: *J. Am. Chem. Soc.* **1974**; 96; 251

/27/ Nafie, L. A.; Keiderling, T. A.; Stephens, P. J.: *J. Am. Chem. Soc.* **1976**; 98; 2715

/28/ Magyarfalvi, G.; Tarczay, G.; Vass, E.: *Adv. Rev.* **2011**; 1; 403

/29/ Kuhn, W.: *Trans. Faraday Soc.* **1930**; 26; 293

/30/ Paterlini, M. G.; Freedman, T. B.; Nafie, L. A.: *Biopolymers* **1986**; 25; 1751

/31/ *Picture taken from:* http://www.bruker.com/industries/pharmaceutical-research-for-pharmaceuticals-and-biopharmaceuticals/quality-assurance/vibrational-circular-dichroism/secondary-structure-of-proteins-and-peptides.html; 2014/08/02 at 3.07 pm.

/32/ Kubelka, J.; Keiderling, T. A.: *J. Am. Chem. Soc.* **2001**; 123; 12048

/33/ Bouř, P.; Keiderling, T. A.: *J. Am. Chem. Soc.* **1993**; 115; 9602

/34/ Atkins, P. W.; Barron, L. D.: *Mol. Phys.* **1969**; 16; 453

/35/ Barron, L. D.; Bogaard, M. P.; Buckingham, A. D.: *J. Am. Chem. Soc.* **1973**; 95; 603

/36/ Nafie, L. A.: *Ann. Rev. Phys. Chem.* **1997**; 48; 357

/37/ Che, D.; Hecht, L.; Nafie, L. A.: *Chem. Phys. Lett.* **1991**; 180; 182

/38/ Barron, L. D. in *Molecular Light Scattering and Optical Activity 2nd Ed.*; Cambridge University Press; **2004**

/39/ Weymuth, T.; Jacob, R. C.; Reiher, M.: *ChemPhysChem* **2011**; 12; 1165

/40/ Hecht, L.; Philips, A. L.; Barron, L. D.: *J. Raman Spectrosc.* **1995**; 26; 727

/41/ Hudecová, J.; Bouř, P.: *Chemické Listy* **2014**; 108; 285

/42/ House, J. E. in *Inorganic Chemistry*; Elsevier, Inc.; **2008**

/43/ Vicentini, G.; Zinner, L. B.; Zukerman-Schpector, J.; Zinner, K.: *Coor. Chem. Rev.* **2000**; 196; 353

/44/ Tsukube, H.; Shinoda, S.: *Chem. Rev.* **2002**; 102; 2389

/45/ Moeller, T.; Martin, D. F.; Thompson, L. C.; Ferrus, R.; Feistel, G. R.; Randall, W. J.: *Chem. Rev.* **1965**; 65; 1

/46/ Werts, M. H. V.; Duin, M. A.; Hofstraat, J. W.; Verhoeven, J. W.: *Chem. Comm.* **1999**; 799

/47/ Mayo, B. C.: *Chem. Soc. Rev.* **1973**; 2; 49

/48/ Cockerill, A. F.; Davies, G. L. O.; Harden, R. C.; Rackham, D. M.: *Chem. Rev.* **1973**; 73; 553

/49/ Parker, D.: *Chem. Rev.* **1991**; 91; 1441

/50/ Horrocks, W.; Sudnick, D. R.: *Acc. Chem. Res.* **1981**; 14; 384

/51/ Tsukube, H.; Shinoda, S.; Uenishi, J.; Kanatani, T.; Itoh, H.; Shiode, M.; Iwachido, T.; Yonemitsu, O.: *Inorg. Chem.* **1998**; 37; 1585

/52/ Reuben, J.: *J. Am. Chem. Soc.* **1980**; 102; 2232

/53/ Meskers, S. C. J.; Ubbink, M.; Canters, G. W.; Dekkers, H. P. J. M.: *J. Phys. Chem.* **1996**; 100; 17957

/54/ Ng, J. B.; Shurvell, H. F.: *J. Phys. Chem.* **1987**; 91; 496

/55/ Malinowski, E. R.; Cox, R. A.; Haldna, U. L.: *Anal. Chem.* **1984**; 56; 778

/56/ Barron, L. D.; Mason, S. F. in *Optical Activity and Chiral Discrimination*; p. 219-220; Reidel Publishing Company, **1979**

/57/ Yamamoto, S.; Bouř, P.: *Angew. Chem. Int. Ed.* **2012**; 51; 11058

/58/ Tsukube, H.; Shinoda, S.; Tamiaki, H.: *Coor. Chem. Rev.* **2002**; 226; 227

/59/ Brittain, H. G.; Fineman, R. I.: *Inorg. Chim. Acta* **1984**; 95; 225

/60/ Yang, X.; Brittain, H. G.: *Inorg. Chim. Acta* **1982**; 59; 261

/61/ Yang, X.; Brittain, H. G.: *Inorg. Chem.* **1981**; 20; 4213

/62/ Tsukube, H.; Shinoda, S.: *Chem. Rev.* **2002**; 102; 2389

Svoluji k zapůjčení této práce pro studijní účely a prosím, aby byla řádně vedena evidence vypůjčovatelů.

JMÉNO	ČÍSLO OP	DATUM	POZNÁMKA